Aus dem Institut der Radiologie
der Medizinischen Fakultät Charité – Universitätsmedizin Berlin

DISSERTATION

Inflammation and mechanical injury as possible reasons for chronic graft failure: A histological analysis of chrome-cobalt stent grafts in the sheep aorta

zur Erlangung des akademischen Grades
Doctor medicinae (Dr. med.)

vorgelegt der Medizinischen Fakultät
Charité – Universitätsmedizin Berlin

von

Luise Kraas

aus Hamburg

Datum der Promotion: 12.09.2014

Table of contents

Abbreviations

AA	Aortic aneurysm
AAA	Abdominal aortic aneurysm
CMSG	Custom made stent graft
CSG	Commercially built stent graft
EVAR	Endovascular aneurysm repair
F	French catheter size
FBGC	Foreign body giant cells
FBR	Foreign body reaction
HES	Hematoxylin-eosin-saffron
HPF	High power field
IFN	Interferon
IL	Interleukin
LGC	Langhans giant cell
MGC	Multinucleated giant cell
MMP	Matrix metalloproteinase
OR	Open surgical repair of aneurysm
ROI	Regions of interest
SD	Standard deviation
TAA	Thoracic aortic aneurysm
TAAA	Thoracic abdominal aortic aneurysm
TEVAR	Thoracic endovascular aneurysm repair
TIMP	Tissue inhibitor of metalloproteinases
TNF	Tumor necrosis factor
WHPS	Weigert-hematoxylin-phloxine-saffron

1 Abstract

1.1 Abstract English

Introduction

Abdominal and thoracic aneurysms have a rising prevalence due to demographic changes. Patients undergoing elective surgery often present with multiple comorbidities. Endovascular aneurysm repair using stent grafts is an attractive, minimally invasive, alternative to conventional open repair but regular radiological surveillance is necessary since long-term stent graft failure can occur years after implantation.

Objectives

Test the safety and biocompatibility of a chrome-cobalt custom made stent graft at 6 months implantation in the thoracic and abdominal sheep aorta.

Methods

Stent grafts were analyzed radiologically and macroscopically for patency, stenosis and migration *in situ*. Microscopic cross sections were stained with hematoxylin-eosin, Weigert hematoxylin-phloxine-saffron and immunohistochemically for CD3+ T-lymphocytes to assess the chronic foreign body reaction, neointima formation, media atrophy, angiogenesis and inflammatory reaction.

Results

Radiologic and macroscopic evaluation showed no significant changes such as endoleakage, migration or occlusion and found only slight scalloping. Microscopy analysis showed significant neointima hyperplasia (mean± SD) in the abdominal (intima: 19.5 ±9.3 µm vs. neointima: 347.8 ±212.8) and the thoracic aorta (intima: 16.3 ±8.7 µm vs. neointima 359 ±117.8 µm) and a significant media reduction in the abdominal (352 ± 85 µm) and thoracic (1453± 519 µm) parts bearing the stent graft when compared to non-stented controls from the same sheep (abdominal: 581 ± 181 µm; thoracic: 2205± 391µm). Trend analysis showed that media changes could correlate with a higher rupture score, changes in the media lamella unit structure and higher CD3+ cell counts, while neointima hyperplasia could correlate with angiogenesis but not rupture. Interestingly, the inflammatory reaction pattern depended more on the animal-specific, healthy intima and media thickness than on the stent diameter or stent/ vessel ratio. This might demonstrate the importance of genetic and developmental factors on inflammatory response in every individual after stent grafting.

In addition, all stents showed multinucleated foreign body giant cell granulomas and secondary Langhans-type granulomas covering the stent surface, demonstrating an ongoing, chronic inflammation driven by innate and adaptive immunity.

Conclusion

This aortic animal model evaluated the safety and biocompatibility of a long-term chrome-cobalt stent graft and identified chronic inflammation of the foreign body type and atrophic media rupture due to chronic mechanical injury as the main risk factors for long-term stent failure.

Keywords:

EVAR, vascular healing, stent graft failure, animal model aortic aneurysm

1.2 Abstrakt deutsch

Einführung

Die weltweite Prävalenz des abdominellen und thorakalen Aortenaneurysmas steigt durch zunehmendem demographischen Wandel sowie Veränderungen des Lebensstiles. Die betroffenen Patienten haben häufig mehrere Komorbiditäten und die endovaskuläre Aneurysmentherapie stellt daher eine attraktive, weil minimal invasive, Therapiealternative zur elektiven Laparotomie oder Thorakotomie dar. Allerdings ist eine regelmäßige radiologische Nachsorge notwendig, da auch Jahre nach Implantation ein spätes Stentgraftversagen möglich ist.

Studienziel:

Die Langzeituntersuchung von Sicherheit und Biokompatibilität eines chrome-kobalt Stentgrafts nach sechs Monaten Implantation in die thorakale und abdominale Schafaorta.

Methoden:

Sechs Monate nach Implantation wurden die Stentgrafts radiologisch und makroskopisch *in situ* auf Migrations- und Durchflussverhalten geprüft. Mikroskopische Schnitte wurden mit Hämatoxylin-Eosin, Weigert Hämatoxylin-Phloxin-Safran und anti-CD3 Antikörpern gefärbt um die Fremdkörperreaktion, die Neointimahyperplasie, Mediaatrophie, Angiogenese und die allgemeine Entzündungsreaktion nach der Stentimplantation zu studieren.

Resultate

Die radiologische und makroskopische Untersuchung zeigte bis auf ein leichtes Scalloping keine Veränderungen der Aorta nach Stentgraftimplantation. Die mikroskopische Untersuchung zeigte eine signifikante Neointimahyperplasie (Mittelwert± Standardabweichung) in der abdominellen (Intima: 19.5 ±9.3 µm vs. Neointima: 347.8 ±212.8) und thorakalen Aorta (Intima: 16.3 ±8.7 µm vs. Neointima 359 ±117.8 µm) sowie eine signifikante Reduktion des Mediadurchmessers in den abdominellen (352 ± 85 µm) und thorakalen (1453± 519 µm) Abschnitten der Aorta, in die das Stentgraft implantiert worden war, im Vergleich zu den Abschnitten ohne Stentgraft (abdominell: 581 ± 181 µm; thorakal: 2205± 391µm). Eine vorläufige Trendanalyse zeigte, dass die Mediaveränderungen mit einem höheren Rupturrisiko, Veränderungen in der Media-Lamellen Anordnung und stärkerer CD3+ Infiltration korrellierten, während Neointimahyperplasie zwar mit Angiongenese jedoch nicht mit einem höheren Rupturwert korreliert werden konnte. Interessanterweise zeigte sich,

dass das individuelle Entzündungsprofil mehr von dem gesunden Intima- und Mediadurchmesser als vom Stentgraftdurchmesser oder dem Verhältnis von Stentgraftdurchmesser zum Gefäßdurchmesser abhing. Möglicherweise haben genetische und epigenetische Entwicklungsfaktoren einen entscheidenden Einfluss auf die individuelle Entzündungsreaktion nach Stentgraftimplantation.
Die an allen Stentgrafts beschriebenen Fremdkörpergranulome und Langhans-typ Granulome zeigten, dass an der Stentgraftoberfläche eine andauernde, chronische Entzündungreaktion mit Anteilen des angeborenen und adaptiven Immunsystems stattfand.

Schlussfolgerung:

Die Langzeituntersuchung der Sicherheit und Biokompatibilität der Aortenveränderungen nach Implantation des untersuchten chrome-kobalt Stentgrafts identifizierte eine chronische Entzündung mit Fremdkörperreaktion und die Atrophie und Ruptur der Media durch chronische, mechanische Schädigung als Hauptrisikofaktoren für das Langzeitversagen von Stentgraftimplantaten in der Aorta.

Stichwörter:

EVAR, vaskuläre Therape, Stentgraftversagen, Mediaatrophie, Tiermodell, Aortenaneurysma

2 Introduction

2.1 Aortic Aneurysm

2.1.1 Definition

Aortic aneurysm is defined as a pathological, permanent dilatation of the aortic lumen (Maier, Gee et al. 2010). The healthy human aortic diameter ranges from 3.5 cm in the thoracic part to 2.5 cm in the abdominal part. Exceeding these diameters by 150% is commonly considered pathologic (Wanhainen 2008).

The healthy aorta consists of three different layers the inner intima, the media and the external adventitia (see Fig. 1).

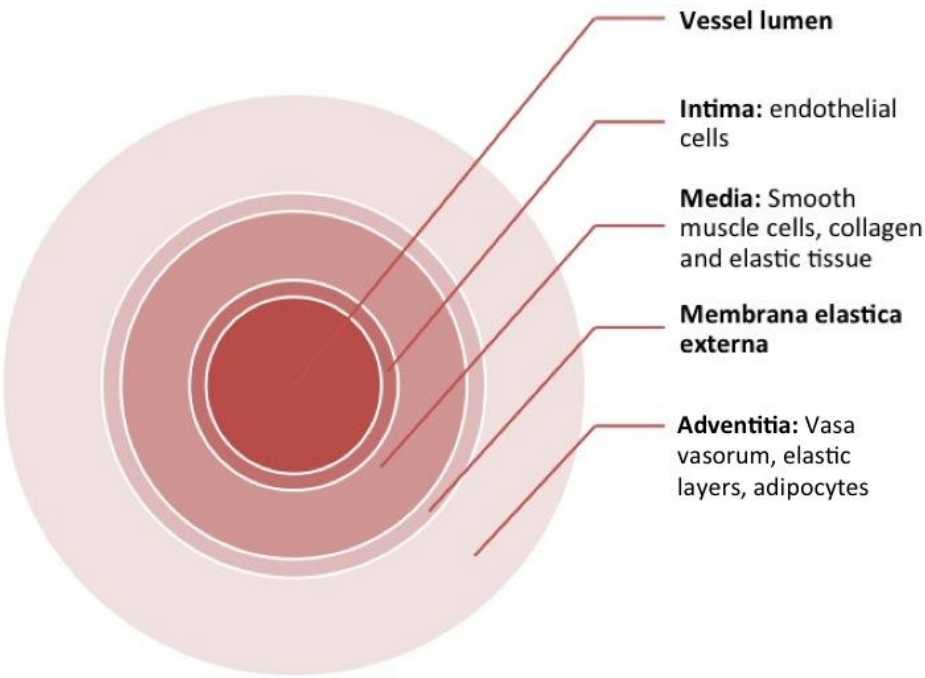

Fig. 1 Schematic layers of the aortic wall.

In the wall of an AA, the relation of these layers and their structure is fundamentally changed. In recent years, many reports have found aortic aneurysm to be a complex multifactorial disease involving an imbalance between the degradation of elastic tissue via matrix metalloproteinases (MMPs), immature neovascularization and angiogenesis and inflammation-driven intima plaque formation (Pearce and Shively 2006, Reeps, Pelisek et al. 2009). Changes in blood flow patterns due to dilatation lead to mechanical stress and localized damage of the weakened aneurysm wall. The risk of aneurysm wall

rupture is consequently directly related to the aneurysm size, its annual increase growth and symptoms (Golledge, Muller et al. 2006).

2.1.2 Classification

Aortic aneurysms can be classified according to their anatomical localization into thoracic aortic aneurysm (TAA), abdominal aortic aneurysm (AAA), which account for 85% of all aortic aneurysm, and thoracic abdominal aortic aneurysm (TAAA).
Several other classifications coexist, based on the extent of the aneurysms (aneurysm verum, spurium, dissecans)(Mehrpooya, Salehi et al. 2012), morphology (fusiform, sacciform)(Pappu, Dardik et al. 2008) or etiology (degenerative/atherosclerotic, genetic, infective, congenital, inflammatory) (Creager and Loscalzo 2008).

2.1.3 Epidemiology

International screening results estimate that AAA is prevalent in 5 to 7% of over 50-year-old persons (Lindholt 2001, Lindholt 2003) and the tenth most common cause of mortality (Golledge, Muller et al. 2006). For TAA a prevalence of 450 per 100,000 persons is estimated based on autopsy results of the Swedish population between 1958 and 1985 (Svensjo, Bengtsson et al. 1996).
Several risk factors have been associated with the development and the progressive dilatation of aortic aneurysm (Table 1).

Table 1 Risk factors associated with Aortic Aneurysm in 9 Population Screening Studies

Risk factors	Weighted mean (for age > 50years)	CI
Smoking	2.77	(2.48-3.10)
Family history	1.99	(1.61-2.46)
CHD	1.84	(1.68-2.02)
Cholesterol	1.37	(1.26-1.49)
Hypertension	1.35	(1.24-1.46)
Female	0.27	(0.23-0.31)
Black Race	0.67	(0.54-0.82)
Diabetes	0.67	(0.58-0.77)

CI= Confidence interval; CHD= Cardiovascular Heart Disease, defined as history of myocardial infarction and/or angina (3313 AAA detected in 111101 screened) Weighted means for % aneurysm and for odds ratio are combined overall effect assuming fixed effects; This table is adapted from Golledge, Muller et al. 2006.

Aortic aneurysm is associated with age and several other risk factors for the development of cardiovascular diseases such as nicotine abuse and dyslipidemia. Through growing life expectancy and demographic change in the age pyramid of western societies the prevalence is expected to rise (Howell, Zaqqa et al. 2000, Zankl, Schumacher et al. 2007).

2.1.4 Therapeutic Options

Current therapies of this progressive disease focus on surgical resection of the aneurysm with graft replacement and a medical reduction of risk factors and comorbidities such as arterial hypertension, atherosclerosis, hyperlipidemia, smoking etc. (Golledge and Norman 2011, Le Manach, Ibanez Esteves et al. 2011).

2.1.4.1 Open surgical repair

The classical open surgical resection of the aneurysm requires lateral thoracotomy and use of cardiopulmonary bypass in the case of TAA, or longitudinal laparotomy and aortic clamping for AAA resection. Both interventions are done in the acute emergency of aneurysm rupture but most interventions are done electively if the risk of rupture is estimated to be higher than the complications associated with the interventions (Chaikof, Brewster et al. 2009). The procedure, related complication rates range from 1 to 5% in elective interventions, depending on the patient's comorbidities, the surgery department, the experience (Elkouri, Gloviczki et al. 2004, Golledge, Muller et al. 2006)

2.1.4.2 Endovascular Aortic Repair (EVAR)

In 1991 Juan Parodi described a new technique of abdominal aneurysm repair via the endovascular deployment of a stent graft (Parodi, Palmaz et al. 1991). Endovascular prostheses are deployed across the aneurysm through a catheter-based introducer in such a way that the aneurysm is effectively "excluded" from the circulation with subsequent restoration of normal blood flow.
EVAR was greeted with great enthusiasm by part of the vascular surgeons for its availability as a less invasive aneurysm repair technique even for patients that were unfit for an open surgical procedure due to their severe comorbidities

2.1.4.3 *Short term results of EVAR*

Large randomized trials showed a significant reduction of perioperative mortality and morbidity for EVAR (Elkouri, Gloviczki et al. 2004), (Greenhalgh, Brown et al. 2004, EVAR-TRIAL-1 2005, EVAR-Trial-2 2005, Biancari, Catania et al. 2011).
Three important studies have evaluated the benefits and risks of EVAR for AAA:
DREAM (Dutch Randomized Endovascular Aneurysm Management) (Prinssen, Verhoeven et al. 2004).
EVAR trial 1: Endovascular aneurysm repair versus open repair in patients with abdominal aortic aneurysm(EVAR-TRIAL-1 2005).
EVAR trial 2: Endovascular aneurysm repair and outcome in patients unfit for open repair of abdominal aortic aneurysm: randomized controlled trial (EVAR-Trial-2 2005).

DREAM (351 patients enrolled) and EVAR trial 1 (1082 patients enrolled) published encouraging results on short term mortality: Endovascular repair was associated with an improvement in abdominal aneurysm-related survival (4.7% mortality in open vs. 1.7% mortality in EVAR at 30 days) (Greenhalgh, Brown et al. 2004). DREAM confirmed these findings with a 30-day mortality of 4·6% for open repair versus 1·2% for EVAR. Similar encouraging short-term results have been observed for the endovascular treatment of thoracic aneurysm (TEVAR) for TAA and thoracoabdominal aortic aneurysm (TAAA) (Greenberg, Lu et al. 2008). On the other hand these first larger trials all reported much higher reintervention rates, due in part to newness of this technique, but also to EVAR and TEVAR (thoracic endovascular aneurysm repair) imminent problems such as secure anchoring and secure aneurysm occlusion without leakage (Greenhalgh, Brown et al. 2004, EVAR-TRIAL-1 2005, EVAR-Trial-2 2005).

2.1.4.4 *Long-term results of EVAR*

But EVAR-1 also found that, 4 years after randomization, all-cause mortality was similar in the open surgical and endovascular treatment group of AAA and that the proportion of patients with postoperative complications was 41% in the EVAR group compared to 9% in the open repair group (EVAR-TRIAL-1 2005). Rapid development and continuous innovation of this technique have reduced the reintervention rate to be almost as low as the open repair (OR) reintervention rates (when OR-related hernia is included in the statistics (Lederle, Freischlag et al. 2012)).

Most importantly, long-term follow up refuted one of the central assumed advantages of EVAR showing that *“[…] endovascular repair led to increased long-term survival among younger patients but not among older patients, for whom a greater benefit from the endovascular approach had been expected [...]“* (Lederle, Freischlag et al. 2012).
The recently published results indicating a superiority of EVAR in younger patients stress the importance of long-term patency of endovascular grafts.
In the literature the reported frequency of late EVAR failure ranges from 0.7% to 3.3% (Harris, Vallabhaneni et al. 2000, Forbes, Harrington et al. 2012). Since the durability of the newer stent grafts for long-term use in younger patients is not yet known, foreign body reactions need months to years to be established (e.g. in tuberculosis) and most comparative experimental animal models use only 3 month for assessment of aortic ingrowth, the study planned the implantation of the stent grafts for a longer period (6 month) focusing especially on the role of the chronic foreign body reactions and the correlation with stent function.

2.1.5 Complications of EVAR

Endovascular repair faces particular concerns regarding the durability of the anchoring system and aneurysm expansion. Aneurysm expansion may result from perivascular leaks, which are a unique complication of endovascular stent grafts. Fig. 2 illustrates the four different types of endoleaks.
Perivascular leaks may result from an incompetent seal at one of the graft attachment sites (Endoleak Type I or IV), perforation of graft fabric (II, Fig. 2) or blood flow in aneurysm tributaries (III Fig. 2), which would usually be ligated during open surgery.

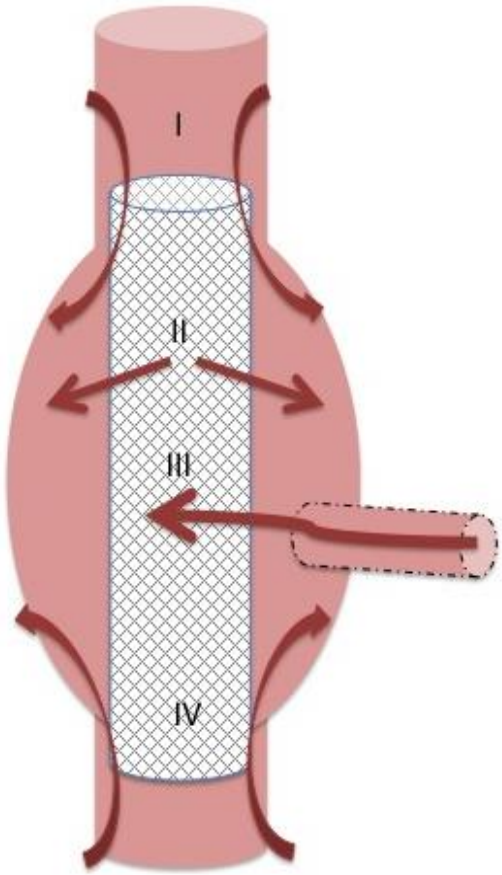

Fig. 2 Four Different types of endoleaks after endovascular aneurysm repair: Type I endoleaks are due to incompetent seal at the proximal aortic neck, Type II due to leaking or rupture of graft fabric, Type III due to blood flow in aneurysm tributaries and Type IV due to incompetent seal at the distal stent end. (Red arrows depict the direction of blood flow.)

2.2 Stent grafts

Several different stent-grafts are currently available and commercially used:

- Straight grafts, in which both ends are anchored to the infrarenal aorta;
- Bifurcated grafts, in which the proximal end is anchored to the infrarenal aorta and the distal ends are anchored to the iliac arteries;
- Fenestrated grafts, which are designed with openings in the wall that can be placed across the renal or celiac arteries while still protecting vessel patency through these critical arteries.

In addition, extensions can be placed from inside the main endograft body into the visceral arteries to create a hemostatic seal. Several modular stent graft systems have been developed to increase the eligibility for endovascular treatment with commercially available stent-grafts (Jayia, Constantinou et al. 2013) which is often constrained by

anatomical conditions to 50 to 30% of open repair (Koskas, Cluzel et al. 1999, Guivier-Curien, Deplano et al. 2009, Singland, Mitton et al. 2010).

At the department of vascular surgery, Hôpital Pitié-Salpêtrière, Paris, this has led to the development of a custom-made stent graft (CMSG), that has successfully passed preclinical and clinical trials (Koskas, Brocheriou et al. 2005, Singland, Mitton et al. 2010)and obtained approval from the French authorities (AFNOR NF EN ISO 14630, 12006-2, 12006-3, 14299). The Laboratory of Vascular Implants, Hôpital Pitié-Salpêtrière published the stent graft fabrication and its internal and external validation and control measures in 2005 (Koskas, Brocheriou et al. 2005).
Until today more than 440 patients (Guivier-Curien, Deplano et al. 2009) have successfully undergone endovascular repair with a CMSG produced by the Laboratory of Vascular Implants made of a 316 L stainless steel alloy, uncrimped woven polyester and suture.

2.2.1 Stent materials

There are many different materials and finishings used to produce stent alloys in vascular surgery. These differ in their biomechanical characteristics such as stress and strain resistance and elasticity but alloys vary in biocompatibility and cost. Among the first and most widely used materials was stainless steel, which combined a high mechanical stability with a high radioopacity thereby allowing for a good radiological follow-up.
In vascular surgery the stiffness of the material can lead to vessel injury and as corrosion. The industries have therefore continuously developed new materials (e.g. nitinol stents or tantalum stents). For our experiments we were especially interested in chrome-cobalt stents that allow for finer struts to exercise the same amount of radial force and longitudinal stability (Alicea, Aviles et al. 2004). The stent used in this experiment also had tungsten finishing which enhances radioopacity. (Alicea, Aviles et al. 2004)

2.3 Foreign body reaction (FBR)

Foreign body reaction can be divided into an acute phase and a chronic phase (Anderson and Miller 1984, Anderson, Rodriguez et al. 2008).
Initially the insertion of a foreign body e.g. the implantation of an endovascular stent graft leads to an acute inflammatory reaction and exudate of blood into the surrounding tissue. In the vessel driven by IL-1ß, TNF-alpha, IL-6 blood monocytes turn into activated macrophages and start to adhere to the material.
Then, in a complex pattern of mutual cytokine regulation and production (Jones, Chang et al. 2007) involving mast cells and polymorphonuclear cells and IL-4 and IL-13, the acute inflammation becomes chronic, lasting for around 3 weeks in *in vitro* studies (Anderson, Rodriguez et al. 2008).
This group states that these stimuli lead to macrophage differentiation via their partial alternative activation, resulting in mannose receptor upregulation. Lymphocyte infiltration in this chronic phase shows a switch towards a T_H2 cytokine profile with the continuous secretion of IL-4 and IL-13 as well as granulation tissue formation with fibroblast activation and proliferation. The fibrous capsule formation, angiogenesis and extracellular matrix remodeling have recently been shown to be mast cell dependent via secretion of the extracellular proteoglycan perlecan and fragmentation into fragments containing the endorepellin C-terminal region (Jung, Lord et al. 2013).
Additionally, IL-4 and IL-13 facilitate the fusion of macrophages into foreign body giant cells (Dugast, Gaudin et al. 1997).
The first person to describe in detail the formation of multinucleated giant cells (MGC) was Thomas Langhans in 1868 studying granuloma formation in tuberculosis. In his publication „Über Riesenzellen mit wandständigen Kernen in Tuberkeln und die fibröse Form des Tuberkels“ (Langhans 1868) he differentiates several morphological types and remarks on the apparent interactions with fibrous and spindle-shaped cells leading to their formation. Since then his speculations on the formation of these giant cells through the fusion of mononuclear cells were experimentally confirmed *in vitro* (Anderson and Miller 1984, Most, Spotl et al. 1997, Anderson, Rodriguez et al. 2008).
Multinucleated giant cells are today differentiated histologically into Langhans-type (LGC) and foreign-body-type multinucleated giant cell (FBGC) by the number and arrangement of their nuclei, with the LGC showing an arcuate nuclei arrangement and the FBGC a random arrangement of nuclei.

3 Scientific question

This investigation was part of a larger study named „Clearpass“ which was started in 2007 at the Institute of Vascular Implants, Paris, France. The aim of the study is to produce customized stent grafts using a chrome-cobalt L605 stent and combining the stent graft with a computer chip. This chip allows the examiner to measure the arterial tension within the aortic sac with an external receiver, thereby allowing for a much easier surveillance of the operated patient. The form of attachment made it necessary to rely on the CMSGs that have been used in this department for more than 10 years. This investigation was a randomized experimental study designed to assess and evaluate safety, biocompatibility and toxicity of chrome-cobalt stent grafts 6-months after implantation in an animal model. In particular the neointima formation and vessel wall reaction to the stent graft were analyzed.

4 Material and methods

4.1 Study design

For this study 20 CMSGs were assembled according to published methods (Koskas, Brocheriou et al. 2005) at the Laboratory of Vascular Implants. They were then randomly assigned for implantation into the thoracic and abdominal aorta of 10 female sheep (Fig. 3). After 6 month the sheep were sacrificed after *in situ* analysis. The stent grafts and the aorta were explanted and processed for further histological analysis assessing ingrowth, safety and biocompatibility of the stent grafts in the sheep aorta.

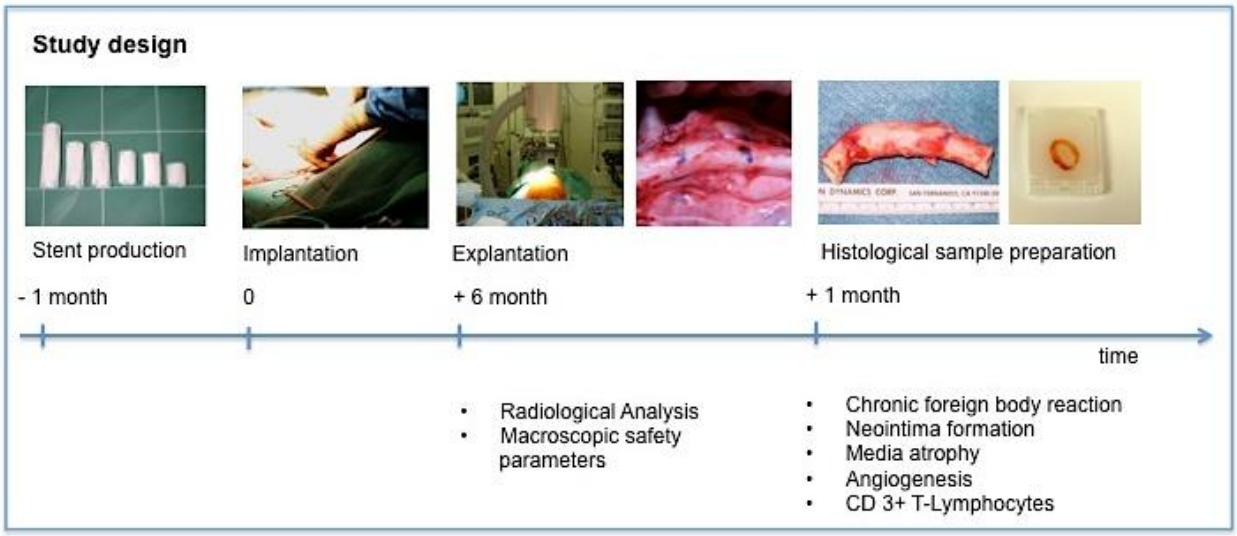

Fig. 3 Schematic presentation of the experimental study design and timeline.

4.2 Animal model

In the past, the Laboratory of Vascular Implants has successfully used sheep (prealpine variety) as an animal model to evaluate custom-made aortic stent grafts at 6 months. For this purpose, 10 female sheep of prealpine variety, raised regularly by l´Institut National de la Recherche Agronomique (INRA), were included in the study protocol. Their average weight in September 2007 was 43 kg.

Ethics approval

The use of sheep as a model was approved by the Directeur Scientifique de l´ Ecole de la Chirurgie, rue du Fer à Moulin, Paris, France in conformity with the guidelines specified by the Commission Nationale pour l'expérimentation animale (CNEA) and the Comité National de réflexion éthique sur l'expérimentation animale (CNREEA). They were treated in accordance with the regulations of the French Ministry of Agriculture

and Fisheries (Décret no. 2001-131) and the European Union council directive (EEC86/609 Council Directive).

4.3 Stent grafts

Twenty stent grafts were produced in the Laboratory for Vascular Implants according to a published procedure (Koskas, Cluzel et al. 1999). Ten were designed for implantation in the thoracic aorta and ten were designed for implantation in the abdominal aorta of pre-alpine sheep. Every stent graft was composed of three parts: Stent, polyester graft and suture.

The stent was an auto expandable chrome-cobalt L605 structure made of a circular wire plied in a zigzag pattern (Gianturco arterial Z stent®, Microval, Saint-Just-Malmont, France). This combination is called MAC25SH (CoCr20W15Ni, DIN 2.4964, ISO 5832-5 ASTM F90, UNS R30605) and also marketed under the name of L605 ®- Alloy 25 ®- Alacrite XSH ®.

For the thoracic stent grafts, two stents were strung together at the loopholes of every zigzag angle and fixed with 10 surgical knots using polyester 4/0 Cardioflon (Laboratoires Peters, Bobigny, France). The diameter of all stent grafts was 12 to 14mm and the length was between 37 and 55 mm for the thoracic stent grafts and 18 to 27 mm for the abdominal stent grafts, respectively.

At the extremities of the stent skeleton, a thicker thread (2/0) was filed through the loopholes in order to exert a longitudinal traction. Thereby the diameter of the stents´ skeleton was temporarily reduced and the stentskeleton could be introduced into a plastic tube.

By pulling at the end of these traction threads the stent skeleton was then moved from one end of the plastic tube into a graft of uncrimped woven polyester (Twillweave®, Sulzer Vascutek, Incchinnan, Scotland) with a diameter of 12, 14 or 16 mm. The thickness of this fabric was 0.3mm. The ensemble was then fixed with a sequence of 10 surgeon’s knots at the metallic loops at the extremities of the stents, using polyester 4/0 sutures (Cardioflon, Laboratoires Peters, Bobigny, France). Each surgeon´s knot is composed of two overhand knots turned in opposite directions but with an additional twist taken after the first overhand is tied. Then the border of the uncrimped polyester fabric was trimmed with a high temperature cautery (AA05 Loop Tip 2''Flexable

Extended Shaft, Boovie Medical Corporation, St. Petersburg, Florida, US) to coincide exactly with the length of the stent skeleton.
All stent grafts were produced under a laminar flow unit and underwent wet heat sterilization using steam. Following this sterilization process, the stent grafts were sterilely packaged for transport to the operation room at Fer-à-Moulin, Paris, France.

4.4 Implantation

Implantation of the stent-grafts took place at the Ecole de la Chirurgie, rue du Fer à Moulin in September 2007. All surgical procedures were carried out under standard, aseptic conditions.
Before implantation of the stents, the 10 female sheep received premedication with Nalbuphine 2mg, Cefamandol 750 mg, and 500ml of Bionolyte intravenously. For the general anesthesia, 16 ml of sodium thiopental (Nesdonal®, Specia, Montrouge, France) was administered intravenously at medical induction and 4 ml continuously during the intervention (overall dose 20 ml of sodium thiopental). Then the sheep were placed in supine position on a radiotransparent table. They were orally intubated, mechanically ventilated with oxygen (2,5 l/min) and continuously anesthetized with 1.5% Isoflurane (Furene, Abbott GmbH, Wiesbaden, Germany) and Nitrous oxide (0,25 l/min).
Oxygen saturation, arterial pressure, body temperature and heart rate were continuously monitored throughout the intervention.

Abdomen and groin were shaved and prepped with iodine and draped. The abdominal aortic bifurcation was exposed through a median xypho – pubic transperitoneal laparotomy and punctured. This approach was used for all the sheep except the first one, where a retroperitoneal lobotomy was performed. Through the needle, a J-tipped 0.35“ guide wire was pushed into the aorta under fluoroscopy. A Pigtail Flush 1.7 mm/5 F catheter (Imager II angiographic catheter, Boston Scientific, Natick, US) was then pushed over the wire. An aortography was performed injecting Ioxitalamate (Telebrix 35, Guerbet, Villepinte, France) and using fluoroscopy with a c- arm digital subtraction angiography unit (OEC Diasonics 9600, GE medical worldwide). Then an Amplatz Super Stiff® guide wire (Boston Scientific, Natick, US) was pushed into the sheath. One mg/kg of heparin was given intravenously. Coaxial a 6mm/18 F introducer system

(Keller-Timmermanns®, W.Cook Europe, Bjaeverskov Denmark) was pushed over the guide wire through transverse arteriotomy centered by the puncture site. Then the introducer was advanced under fluoroscopic control into the aorta unto the programmed level for the deployment of the stent graft.

At that point, the stent graft was taken out of its sterile packing (Fig.4A), soaked in Rifampicin for 1 minute and introduced into a metallic cone by pulling at the traction threads (Fig. 4B). These traction threads were then cut and the stent graft advanced into the introducer (Fig 4.C) with the help of a flexible mandrel. Thus loaded, the position of the implantation site was confirmed by arteriography through a left humeral catheter proximal to the deployment site. Then the thoracic stent graft, consisting of two Gianturco stents strung together and covered with a Dacron polyester, was deployed through withdrawal of the introduction sheath under continuous fluoroscopic control (Fig. 4D). In the same manner the monomial abdominal covered stent-graft was implanted in the sub renal aorta. Arteriography was performed at the end of each intervention to ascertain the proper deployment, accurate positioning of the stent-grafts and exclusion of endoleakage.

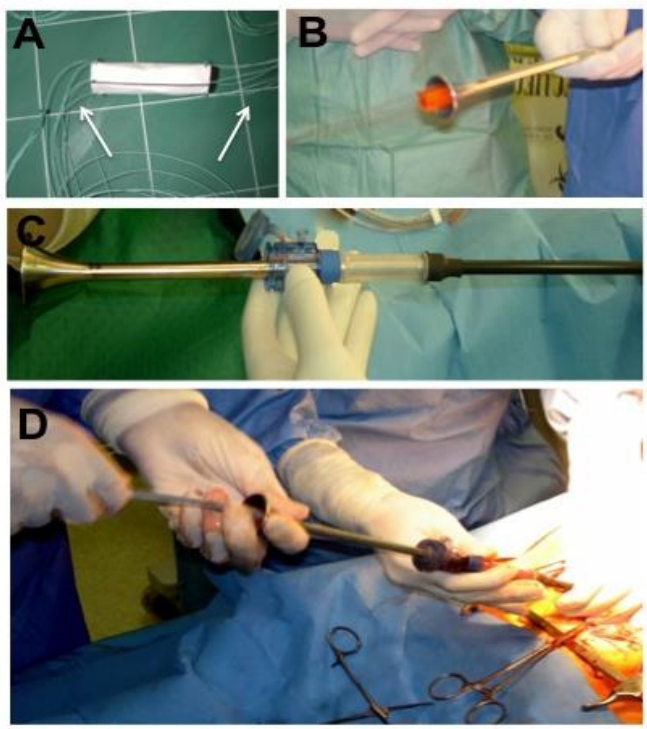

Fig. 4 The implantation procedure: A sample stent graft with traction threads (white arrows); B The Rifampicin-soaked stent graft (orange) is loaded into the metallic cone with the traction threads; C Connection of the metallic cone and the introducer system; D Deployment of the stent graft.

At the end of procedure and after withdrawal of the introducer the arteriotomy was closed through a continuous 6/0 polypropylene suture.
In three cases closing the arteriotomy with continuous suture was impossible (sheep no. 4, 7, 8). In one case (sheep no. 8) a prosthetic enlargement patch was used. In the two other cases (sheep no.4 and no. 7) the terminal aorta was replaced through aorto-aortal bypass with a woven Dacron polyester prosthesis.
Afterwards, the subcutaneous tissues and the skin tissue were closed in layers with a non-resorbable continuous suture.
After awakening and warming, the sheep were kept under surveillance at the Ecole de chirurgie's laboratory stables for 72 hours and administered 750 mg Cefamandol (cephalosporin) and 7 ml Duphapen® (Penicillin) before returning to their previous stables at the INRA, where they spent the following 6 months.

4.5 Explantation

The explantation of all stent grafts took place at the Ecole de la Chirurgie 6 months after implantation. The sheep were premedicaled with 16ml of sodium thiopental (Nesdonal®, Specia, Montrouge, France) at medical induction and received 4ml continuously during the intervention (overall dose 20ml of Sodium thiopental). Then the sheep were placed in supine position on a radiotransparent table. They were orally intubated, mechanically ventilated with Oxygen, (2,5 l/MN) and continuously anesthetized with 1.5% Isoflurane (Furene, Abbott GmbH, Wiesbaden, Germany) and Nitrous oxide (0.25 l/MN).
After shaving, disinfection with iodine and draping a laparotomy was performed. The distal bifurcation of the aorta was explored, prepped/exposed and punctured. Through the needle a J-tipped 0.35“ guide wire was pushed into the aorta under fluoroscopy. A Pigtail Flush 5 F catheter (Imager II angiographic catheter, Boston Scientific, Natick, US) was introduced and pushed through both implanted aortic stent grafts. A biplane control angiogram of both implants was obtained by injecting Ioxitalamate (Telebrix 35, Guerbet, Villepinte, France) and using fluoroscopy with a c- arm digital subtraction angiography unit (OEC Diasonics 9600, GE medical worldwide).
Then the aortic segment of the abdominal stent graft was exposed, inspected beating and photographed *in situ*. The incision was then enlarged to allow a left thoracotomy. The thoracic implantation site was carefully exposed and the beating thoracic stent graft inspected and photographed *in situ*.

Upon return to the abdominal implantation segment, the aorta was ligated and divided two centimeter proximal and distal of the abdominal implant. The same resection was done for recovery of the thoracic stent-graft, simultaneously with the intracardiac administration of a lethal dose of Dolethal® (20% w/v Pentobarbitone Sodium).

Explanted stent grafts were carefully probed and rinsed in a 10% formalin solution. Explants were measured (length and diameter) and stored for a minimum of five days in neutral buffered 10% formalin solution before further analysis in the laboratory of Anatomie et cytologie pathologiques, Head Prof Capron, Hôpital Pitié-Salpêtrière, Paris, France.

4.6 Radiological Analysis

The vascular surgeons of the intervention Rafael Coscas and Professor Fabien Koskas performed analysis of fluoroscopy after the end of all procedures.

4.7 Macroscopic safety parameters

At the department of Anatomie et cytologie pathologiques the twelve stent grafts were macroscopically analyzed in three sessions by two independent observers. The explants were carefully rinsed with PBS, aortic ligatures removed and, after measurement, opened with cobalt pincers. The progress of their macroscopic dissection was photographed at all stages.
The following parameters were examined:

- Aneurysm
- Stenosis
- Thrombus
- Diameter

Aneurysm:
Defined as a loss of vessel wall parallelism, this was assessed through inspection and search for palpable vessel protrusion.

Stenosis:

Longitudinal inspections of the whole explant were taken through the explant and the grade of stenosis was evaluated with a ruler.

Thrombus:

Absence of observable macroscopic adhesions.

Diameter

This parameter was measured in order to assess the graft – vessel ratio and to merge the data with the radiological findings. The aortic diameter (measuring from external layer – external vessel layer) of each aortic explant was measured at least three times at two different points: 0.5 cm proximal of the stent graft and 0.5 cm distal of the stent graft. The stent graft diameter was also measured three times: first at the proximal end of the stent graft and secondly at the distal end of the stent graft.

4.8 Histochemical sample preparation

The samples for the microscopic analysis were obtained from the longitudinally opened explants. Using a sharp blade, three thin tongue-shaped samples were obtained from five different parts of every explant (3 samples x 5 parts x 12 stent grafts= 180).

The 5 different parts were (Fig. 5):

1. Part 1: 1cm proximal of the stent graft transition zone
2. Part 2: proximal stent graft-vessel transition-zone
3. Part 3: central part of stent graft
4. Part 4: distal stent graft-vessel transition-zone
5. Part 5: 1cm distal of the stent graft transition zone

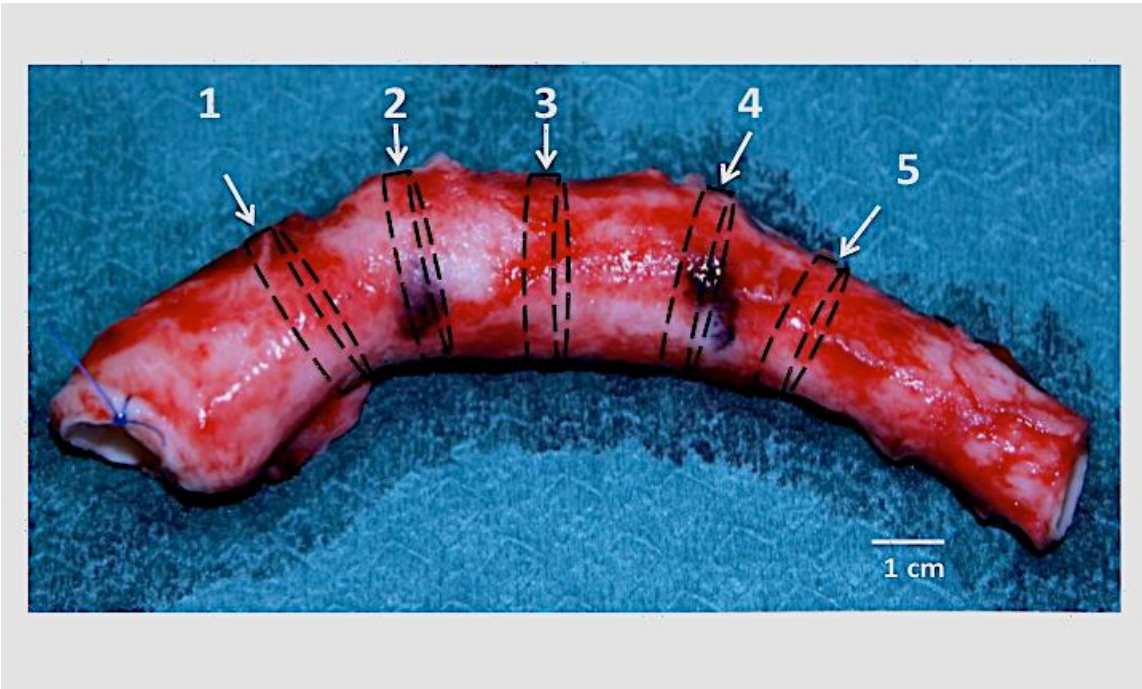

Fig. 5 Exemplary sample of cross sections of the thoracic stent grafts and aorta. Black dashed lines indicate virtual section lines for the different cross sections (white arrows and numbers) from transitional (No. 2+4), central (No. 3) and stent free (No.1+5) parts of a thoracic aorta.

The samples were fixed in 10% buffered neutral formalin, then processed into paraffin blocks, and stored at room temperature. They were cut in 3 mm thick serial sections (Mikrotom Mikrom HM340 E, Francheville, France), fixed on slides and stained with hematoxylin eosin saffron (HES), which stains nuclei blue/violet, cytoplasm red and collagen yellow/orange. Additionally, all samples were routinely stained with Weigert hematoxylin-phloxine-saffron (WHPS). Weigert´s elastin staining was used to visualize

elastic fibers in dark blue/black. The staining was done according to the standard of good practice in the laboratory of Anatomie et cytologie pathologiques (Attachment 1+2).

4.9 Neointima formation and media changes

Histometric analysis was performed on the HES stained slides of the proximal and distal stent graft - vessel transition zone (Part 2 and 4, Fig. 5) to measure the thickness of the luminal and parietal neointima and media of the stent graft aorta. The intima thickness was measured between the lumen and the media. Medial thickness was measured as the distance between the innermost and outermost elastin layers.

First, 1280x1024 pixel images of the samples were acquired using a digital camera (Nikon DS –5MC, Japan) that was coupled with an optical microscope (Bx51, Olympus, Japan). The images were saved in a BMP format.

Then these calibrated pixel images were analyzed with the Act-2U software (Vers.1.5, Nikon, Japan).

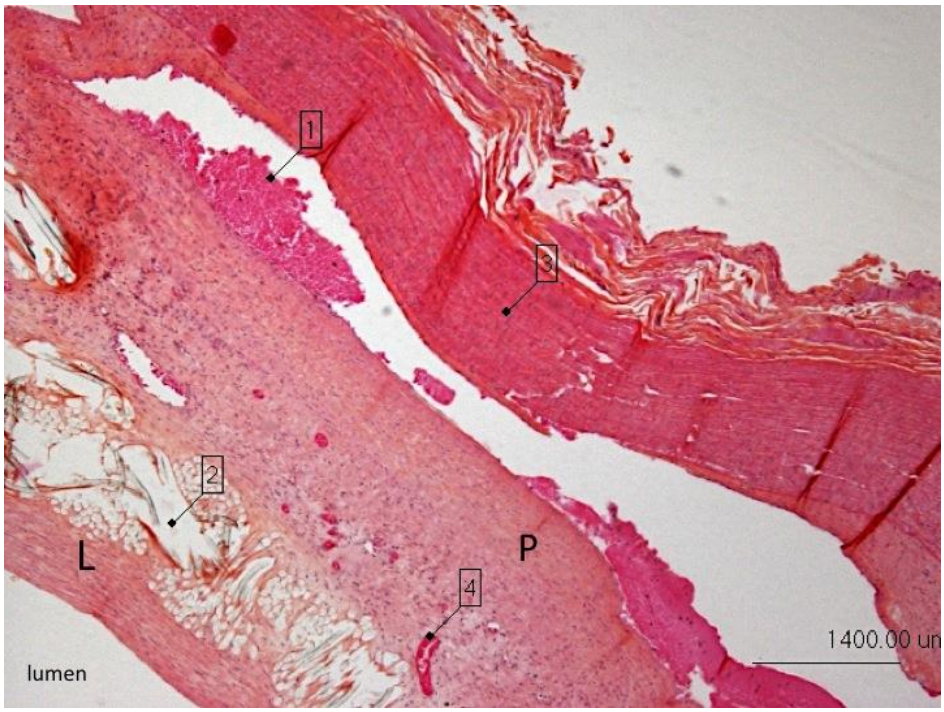

Fig. 6 Overview of histological changes in the aorta 6 month after stent graft implantation. HES stained section of the abdominal aorta; magnification 4x; L=luminal part of the neointima, P=parietal part of the neointima; 1=thrombus between neointima and media; 2= polyester part of the stent graft 3= media; 4= vessel

The measurement was repeated at three different sites for each slide.

The intima and media thickness of the proximal non-stent grafted aorta was measured in the same manner (No. 1 and 5, Fig. 5)

4.10 Semiquantitative analysis of media atrophy

The analysis of the media atrophy was done additionally in a semiquantitative manner calculating a rupture score that was combining two different morphological parameters (rarefaction and loss of undulation, table 2).

For the rarefaction the different the Medial Lamellar Units (MLU) visible in the WHPS staining were counted in the slides of Part 2 (Fig.5) of the explanted aorta The count was done according to published methods (Bashar, Kazui et al. 2002) at 100x magnification. The MLU counting was done at least three times at three randomly selected sites of the aorta proximal to the stent and the stented aorta.

The rarefaction was then calculated into a score ranging from 0-4 with 0= no rarefaction; 1=rarefaction 1-20%; 2= rarefaction 21-40%; 3= rarefaction 41-60 %; 4= rarefaction > 60%.

The loss of undulation was scored ranging from 0-3 (0=no difference between stented/not stented media; 1= almost normal undulation; 2= intermediate undulation; 3= no undulation/flat).

The combination of these two parameters, undulation and rarefaction, resulted in a score according to the system shown in Table 2.

Table 2 Rupture score

Loss of Undulation / Visual rarefaction	0	1	2	3
0	0	0.5	1	1.5
1	0.5	1	1.5	2
2	1	1.5	2	2.5
3	1.5	2	2.5	3

Rupture score combined the visual rarefaction of medial lamellar units with the loss of undulation in the stented aortic media. Rupture score ranging from 0= no rupture to 3= severe rupture of stented aortic media.

4.11 Inflammatory CD3+ lymphocyte response

The aim of immunohistochemistry examination was to qualify and quantify, the extent of mononuclear immune cell infiltration according to established methods in the laboratory (Koskas, Brocheriou et al. 2005). The analysis focused on CD3+ lymphocytes as the one prominent and reliable marker of this immunological response. For this analysis the slides showing the proximal or distal stent-graft vessel transition zone were used.

Antibodies

For immunohistochemistry a polyclonal anti-CD3 antibody (Dako, Glostrup, Denmark) was used at a 1:50 dilution for T-lymphocyte identification, the immunohistochemical processing was done according to established laboratory protocols (Koskas, Brocheriou et al. 2005).

In brief, the paraffin-embedded sample sections were heated in a microwave (900W) twice for 5 minutes in a citrate buffer. To deparaffinize the sections, they were put three times for 5 minutes in xylene, then two times for 5 minutes each in 100% ethanol, twice for 5minutes in 95% ethanol, then 3 minutes in 70% ethanol and finally 3 minutes in ultra pure water.

The deparaffinized sample sections were then incubated for 30 minutes in the prewarmed (98°C) Target retrieval solution ph9 (Dako, Glostrup, Denmark). Then they were left to cool down for 20 minutes at room temperature. After that, they were washed with ultrapure water, then put in 3% H_2O_2 for 5 minutes and washed again with ultrapure water. Next, slides were put in Bluing Buffer (Dako, Glostrup, Denmark) after 5 minutes slides were washed with wash Buffer (Dako, Glostrup, Denmark). Then the slides were incubated for one hour at room temperature with the CD3+ polyclonal antibodies diluted 1:50 . After incubation slides were washed again gently. Next staining was visualized in a two step procedure with the Dako EnVision EnVisionTM+ Dual Link System incubating for 30 minutes at room temperature before additional washing. Then slides were put for five minutes into DAB+ liquid (Dako, Glostrup, Denmark). After washing, Slides were counterstained with aqueous hematoxylin for 1 minute and then rinsed in water. Afterwards slides were put for five minutes into 95% alcohol, then twice for five minutes into 100% alcohol and finally thrice for 5 minutes into Xylene. All preparations were done according to the manufacturer´s guidelines.

4.11.1.1 Immunohistochemical cellcount

After immunohistochemical preparation the processed slides were analyzed microscopically. Because CD3+ T-lymphocyte infiltration was limited to the parietal and luminal neointima, the quantitative analysis defined regions of interest in both neointima parts. The regions of interest were chosen where the positive brown precipitate was strongest at 40 times magnification. The magnification was then changed to 400 times and this was defined as one high power field (HPF). CD3+ lymphocyte cells were counted in 10 connected HPF for the luminal and parietal neointima.

4.12 Angiogenesis

To quantify angiogenesis, two regions of interest (ROI) on WHPS-stained slides of Part 2 (Fig.5) were defined. Vessels were counted in three high power fields at 400 times magnification for each ROI in the neointima.

4.13 Statistical Analysis

The results were calculated using SPSS® statistical software (version 16 for Mac OS X Leopard, SPSS Inc., Chicago, Illinois, USA) and Microsoft Excel for Mac (version 14.2.3.).

Descriptive statistics including the mean, standard deviation and ranges for each group were computed.

When results between abdominal and thoracic position of the stent graft were compared to determine whether significant differences existed between these groups, a Mann-Whitney U-test with a significance level of $P < 0.05$ was performed to evaluate the significance.

To test for differences between the stented and not stented aorta a Wilcoxon Signed Rank test with a significance level of $P < 0.05$ was performed to evaluate the significance.

Due to the small samples size and resulting low power, the analysis of the relationship between different variables could only identify trends for correlations. These trends are presented in a scatterplot with a regression analysis model with $R^2 = 1$ total correlation; $R^2 = 0$ no correlation.

The statistical analysis was done with help from Tibor Schuster from the Institut für Medizinische Statistik und Epidemiologie, Technische Universität München, Munich, Germany.

5 Results

5.1 Study design

This investigation was a part of a larger study named „Clearpass“ that was started in 2007 at the Institute of Vascular Implants. The aim of the study was to analyze the safety and biocompatibility of the assembled stent grafts and to analyze the histological changes in the vessel wall of healthy aorta using sheep as an animal model. In particular the neointima formation and the media changes were analyzed in combination with inflammatory markers of T-lymphocyte infiltration and rupture.

5.2 Animal Model

After the implantation, due to problems mentioned above and detailed below, 4 out of 10 sheep had to be sacrificed prematurely (4/10, 40%). Two sheep were paraplegic on awakening, one developed a bowel ischemia with mesenteric infarction and another one was hemiplegic.

Given the impossibility and cruelty of maintaining these sheep in this setup, they were sacrificed when it became apparent that their disabilities were not transitory.

Complete postmortem analysis was realized in each of these sheep.

Table 3 details the implantation outcome that led to premature sacrifice.

5.3 Stent grafts

Twelve stent-grafts were explanted from 6 sheep (mean weight 43.3 (±6.3) kg) after 6 months duration in the thoracic and abdominal aorta. All harvested stent-graft were macroscopically integral and completely intact without any signs of material fatigue or cracking.

Table 3 Implantation results and adverse events

SHEEP	DEPLOYMENT	DESCRIPTION OF AE	SOLUTION	SACRIFICE
1	Success	——	——	——
2	Success	——	——	——
3	Success	——	——	——
4	Success	Introducer injury	Aorto-aortic bypass	——
5	Success	——	——	——
6	Success	——	——	——
7	Delivery failure of abdominal stent graft	Paraplegia Aortic thrombosis	——	Yes
8	Success	Aortic thrombosis Paraplegia Introducer Injury Closure of arteriotomy difficult	PTFE patch	Yes
9	Success	Hemiplegic Introducer Injury	Aorto-aortic bypass	Yes
10	Success	Bowel ischemia with mesenteric infarction	——	Yes

Table 4 Implantation outcome

IMPLANTATION OUTCOME	**COUNT**
Bowel Ischemia	**1**
Hemiplegia	**1**
Paraplegia	**2**
Introducer Injury	**3**
No complication	**6**

5.4 Implantation

Implantation of the 20 stent-grafts in the aorta of the 10 sheep was technically successful in 19 of 20 cases (95%). Each sheep received one thoracic and one abdominal stent-graft, precisely delivered at the programmed deployment site and without migration. Only in the case of sheep 7 was the deployment of the abdominal stent-graft difficult (1/20; 5%) due to the relatively large diameter of the stent-graft (14mm).

Major difficulties occurred in three sheep during closure of the punctured aortic site (Sheep 4, 8, 9; 30%). Due to the relatively large diameter of the introducer (18 F), the intima of the aorta was injured, necessitating an infrarenal aortic replacement with an aorto-aortic bypass in two cases (sheep 4, 9) and an enlargement of the infrarenal aorta using a thin walled Braun VascuGraft PTFE patch ® (Melsungen, Germany). Sheep 9 was sacrificed due to its hemiplegia. To find the origin of the hemiplegia an autopsy was performed. However, the autopsy could find no cardiac anomaly so paradoxical embolism was unlikely. Since the hemiplegia was most likely due to a cerebral infarctus caused by the catheter manipulation of the thoracic aorta during stent graft implantation. Sheep 10 died of bowel ischemia with mesenteric infarction. The autopsy found inflated, necrotic intestinal loops consistent with this diagnosis, but no signs of stent graft migration or aortic thrombosis. The explanation could be superior mesenteric artery stretching during the implantation procedure.

These sacrificed sheep were excluded from further statistical analysis because the aim of this study was to address the long-term safety and biocompatibility of chrome-cobalt stent grafts, that is after more than 6 months´ implantation.

The great premature loss of 40% of test animals is addressed in greater detail in the discussion.

The remaining six sheep were bred uneventfully at the INRA stables in Jouy-en- Josas, France for six months.

5.5 Explantation

The explantation was successful in all cases. The stent graft was visualized during the operation and the implant could be observed in the beating aorta.

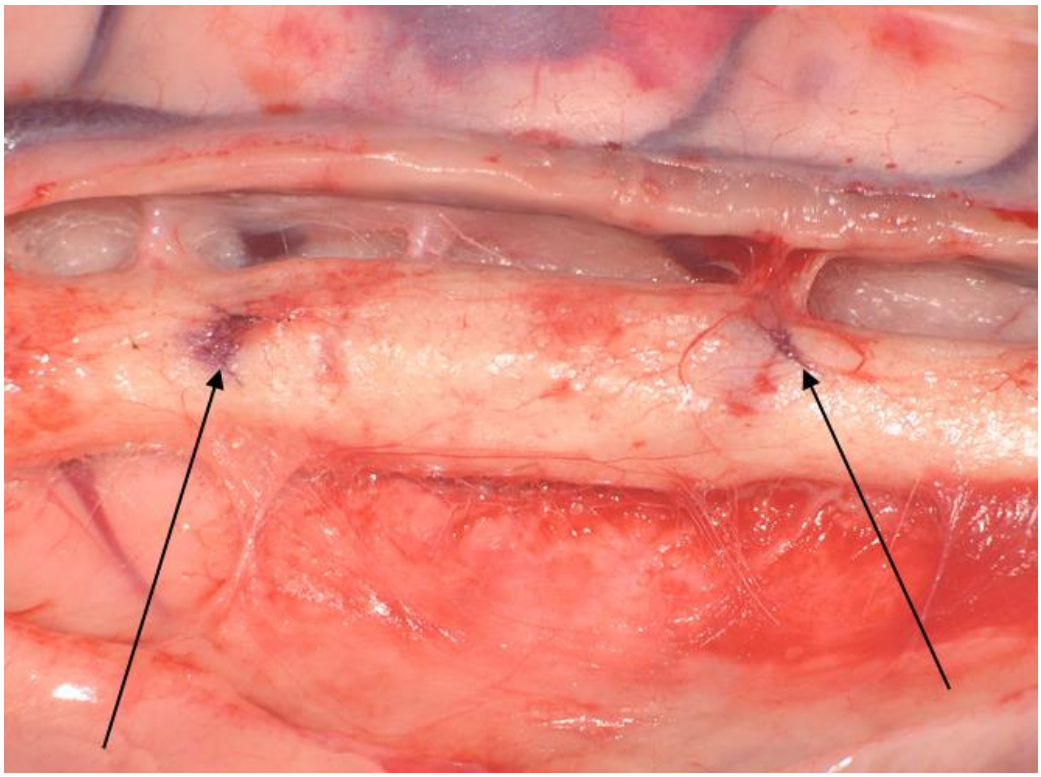

Fig. 7 Thoracic stent-graft *in situ* Photography directly after laparotomy and before explantation of the stent. Black arrows point to the longitudinal outlines of the stent-graft that have been highlighted with a black marker for better visibility on the photography

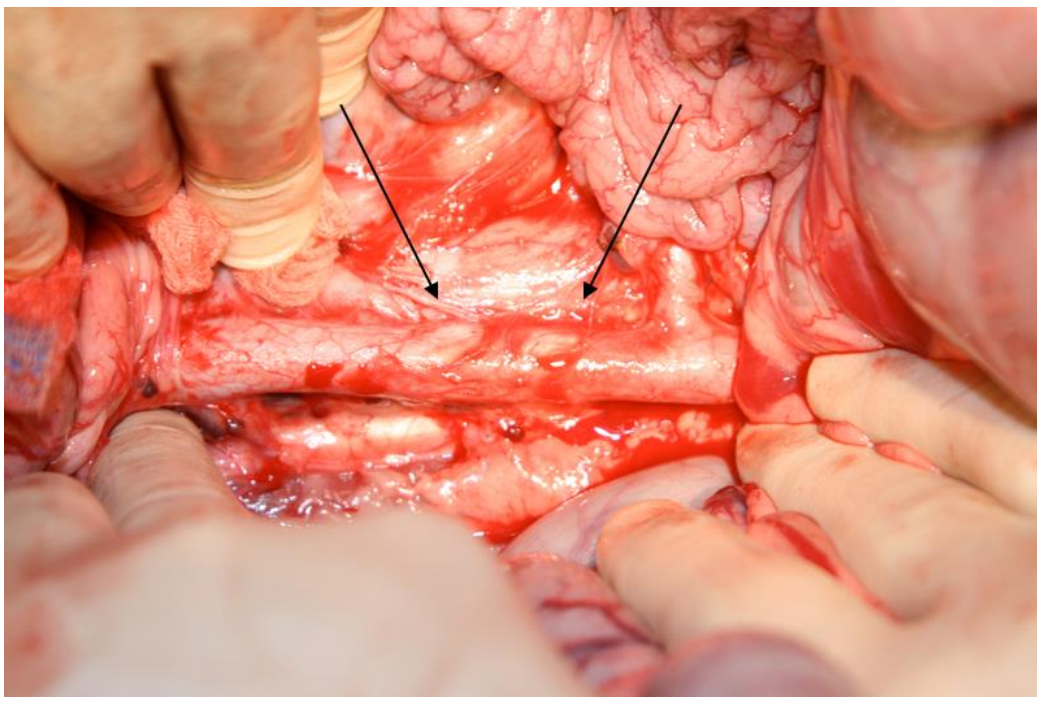

Fig. 8 Abdominal Stent-graft *in situ* Photography directly after laparotomy and before explantation of the stent. Black arrows point to the outlines of the stent-graft that are barely visible without the black marks seen above.

5.6 Radiological Analysis

On the systematic biplane angiograms taken immediately before explantation, none of the twelve stent grafts had migrated from their initial site of deployment or were occluded.

The outline of the radiological image of the stented aorta was in continuity with that of the adjacent non-stented aorta (Fig. 9). Contrast medium went through the stented aorta at the same pace as through the adjacent non-stented aorta.

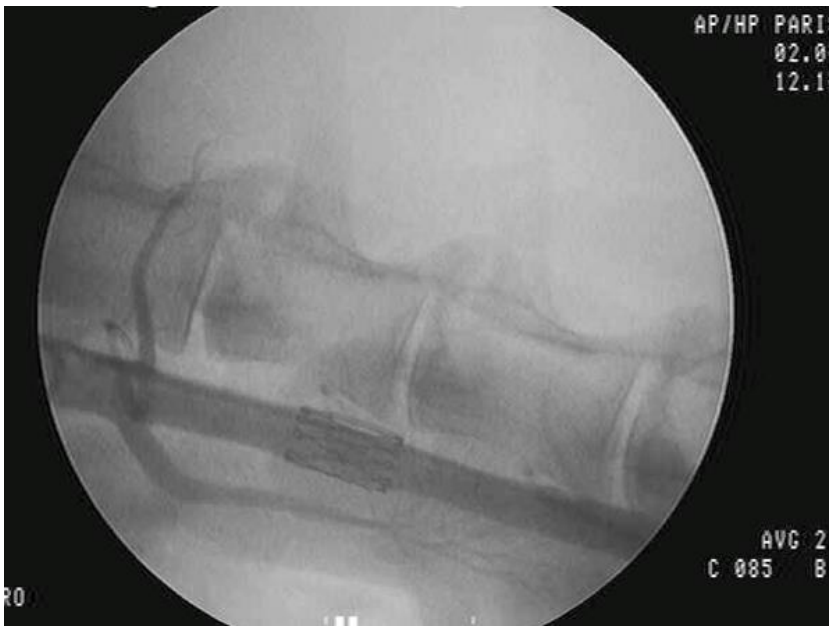

Fig. 9 Angiographic control immediately before explantation

For some stent grafts (sheep 1 and sheep 5 abdominal; sheep 1 and sheep 6 thoracic) where the deployed diameter was clearly larger than that of the implanted aorta, the vessel diameter was narrowed because two adjacent angles of the stent and its oversized membrane protruded into the lumen. This process, also known as scalloping, resulted in a partial stenosis of the vessel. Macroscopic findings (Fig. 10 C) confirmed this. There were no other anomalies at the control angiogram of the twelve implants.

5.7 Macroscopic safety parameters

Aneurysm

When the aortic segment bearing the implant was surgically exposed, the aortic wall was normal over the stent-graft and adjacent to it. There was neither inflammatory reaction nor infection nor aneurysm nor false aneurysm. The presence of the graft was

perceptible *in situ* by palpation and on external inspection because of a distension of the aorta by the implanted stent grafts, especially in the abdominal stent-grafts.

Stenosis

There was no visible stenosis in any of the explanted samples. There was however scalloping observed in some of the thoracic explants due to a mismatch between the stent diameter and the original „natural“ diameter of the aorta in each sheep.

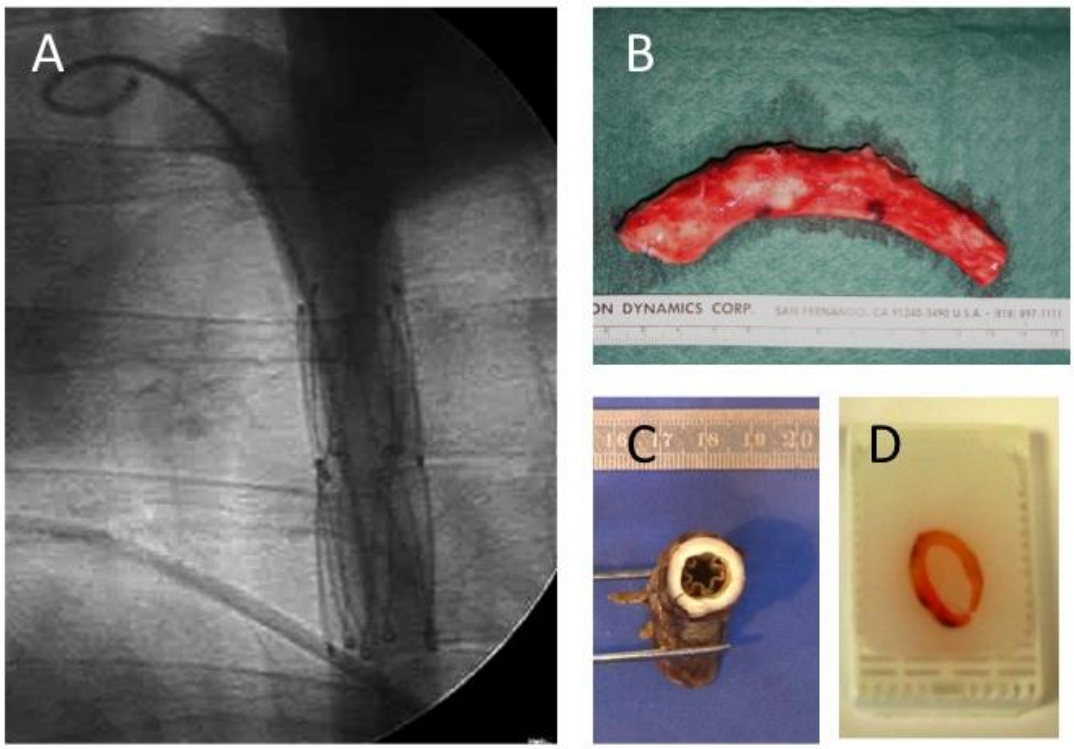

Fig. 10 Gradual analysis of a thoracic stent graft

A detail of the angiography after 6 month implantation; B immediately after explantation; C after preservation in formalin for 8 days; D paraffin embedded section.

Thrombus

There were no macroscopically visible thrombi in any lumen of the twelve explants that remained patent until harvesting. For some particularly over-dimensioned stent grafts, the excess of the polyester membrane scalloped inside the lumen (between the angles of the extremities of the metallic skeleton). There was an adherent thrombus filling the dead space between this scalloping and the end luminal surface aorta it covered.

Diameter

Macroscopically, there was a significant difference found between the measured diameter of the native aortic vessel and the implanted stent graft's diameter and consistent radiological findings of over-dimensioned stent grafts. The mean diameter of the aortic vessel was 11.6 (±4.6 SD) mm while the mean graft diameter was 13.67 (±1.37 SD) mm

5.8 Neointima hyperplasia and media atrophy

The neointima had a luminal part towards the aortic lumen and a medial part between the graft and the vessel media. The neointima had a poor cellular content with fibrous extracellular matrix especially in the luminal part and a fine line of endothelial cells towards the lumen. In the parietal part angiogenesis with multiple small vessel was found predominantly but not exclusively.

5.8.1 Neointima thickness

There was a significant difference between the intima thickness and the neointima thickness measured in the abdominal (intima: 19.5 ±9.3 µm vs. neointima: 347.8 ±212.8) and the thoracic (intima:16.3 ±8.7 µm vs. neointima 359 ±117.8 µm) parts of the aorta (Fig. 11). This was observed in all stent grafts. There was no significant difference between the intima thickness measured in the abdominal or thoracic part of the aorta. Also there was no significant difference between the neointima formation in the abdominal or the thoracic part of the aorta.

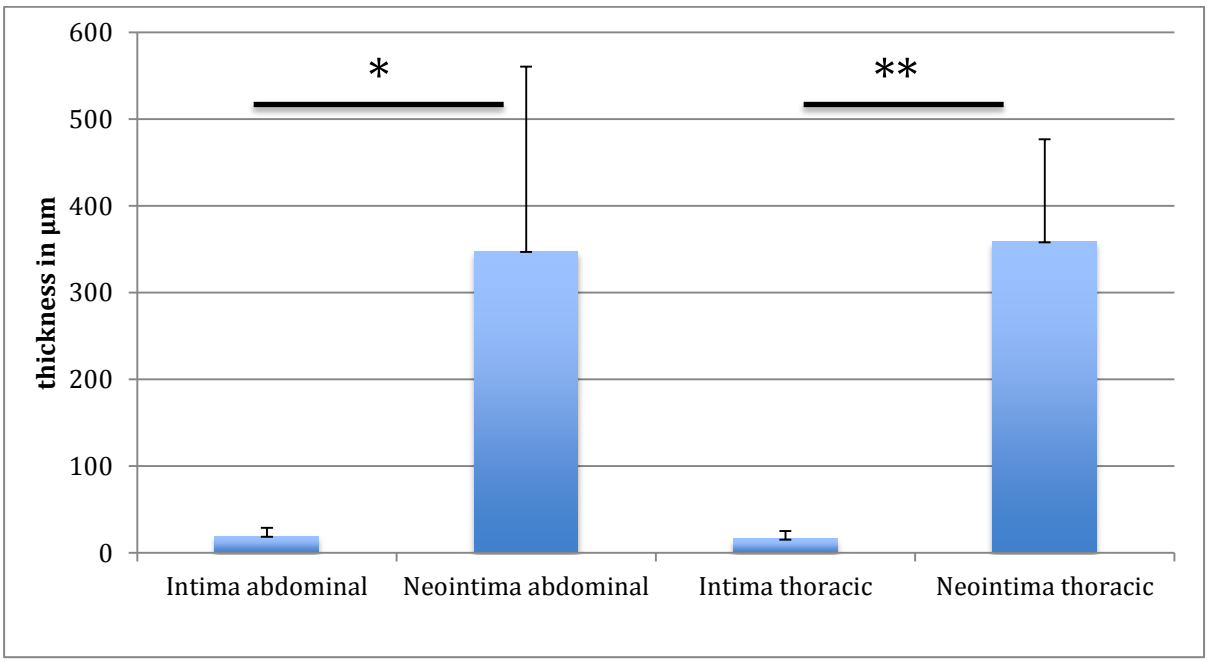

Fig. 11 Intima and neointima thickness in abdominal and thoracic samples. Thickness measured in the stented (neointima abdominal/thoracic) and not-stented aorta (intima abdominal/thoracic);* significant difference p< 0,05, ** p<0,01 , T error bars.

5.8.2 Media atrophy

The media thickness in the stented aorta was reduced in comparison to the thickness of the stent-free aorta. This difference was statistically significant in both the abdominal and the thoracic parts (Fig. 12).

This difference in media thickness was observed in all samples. The media in the stented aorta also showed structural differences and rupture described in 4.9.

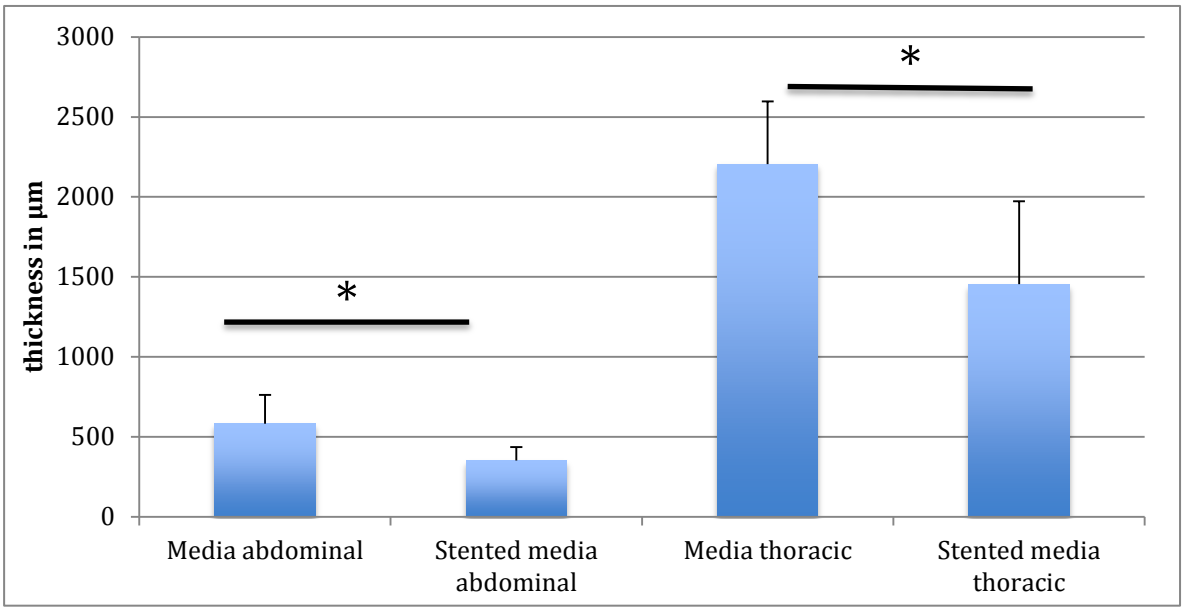

Fig. 12 Significantly reduced thickness in abdominal and thoracic media of stented aorta when compared to non-stented aortic media

Media thickness measured in the stented and not-stented aorta * significant difference $p<0,05$; T error bars.

5.9 Semiquantitative score for media rupture

The elastic fibers of the stented aorta changed their form and rupture and media atrophy was observed (Fig. 13B, D) as compared to non-stented aorta (Fig. 13A, C).

The radial force of the stent graft led to a rarefaction of the MLU in the stent-graft sample. The average calculated rarefaction of MLU was 12 (± 0.13 SD) %.

The resulting rupture score ranged between 0 and 3. For individual values see Table 5.

There was no statistically significant difference between the results of the rupture score in the abdominal and thoracic samples (Fig. 14).

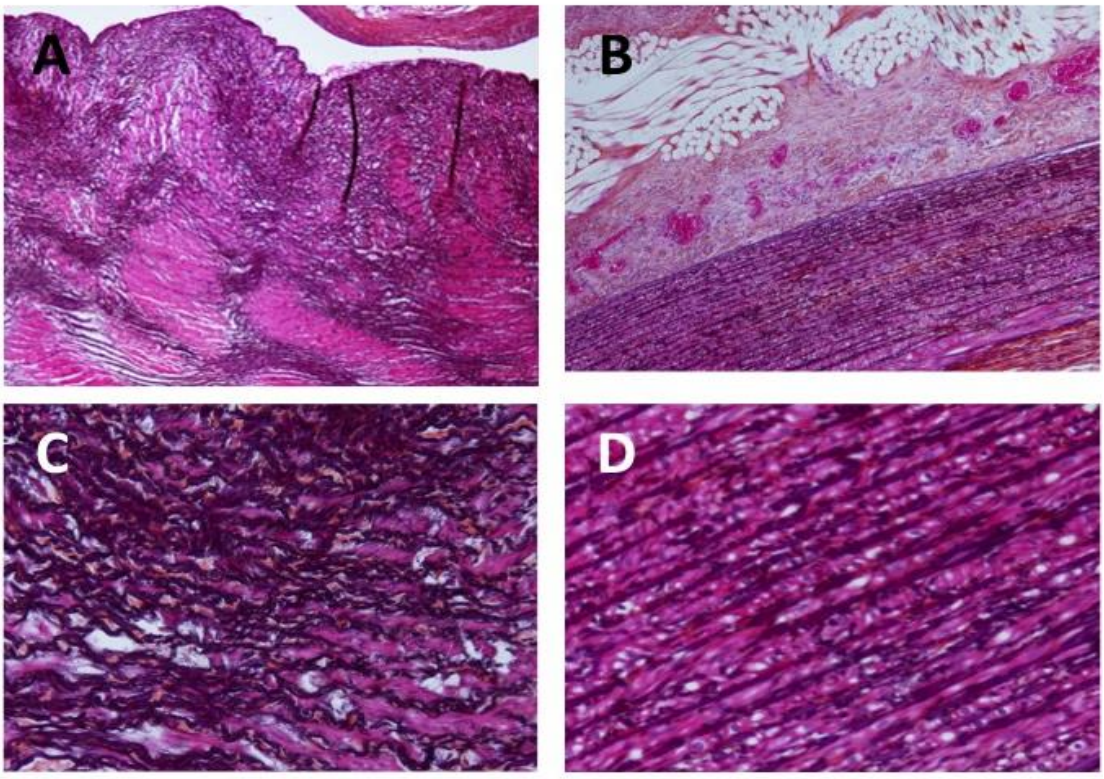

Fig. 13 Representative slides showing the media changes in the thoracic aorta.

A+C: stent graft free media sample; B+D: aortic media with stent graft; A+B at 40x magnification, C+D 400x magnification; WHPS staining

Table 5 Media rupture

Sheep	*Position*	*Rupture score*	*Position*	*Rupture score*
1	Abdominal	1	Thoracic	2
2	Abdominal	1	Thoracic	0
3	Abdominal	2	Thoracic	1
4	Abdominal	2	Thoracic	2
5	Abdominal	3	Thoracic	1
6	Abdominal	0	Thoracic	2

Rupture score ranging from 0 to 3 with 0 = no rupture to 3 = severe rupture

(Rupture defined as loss of MSU and loss of undulation see 3.10)

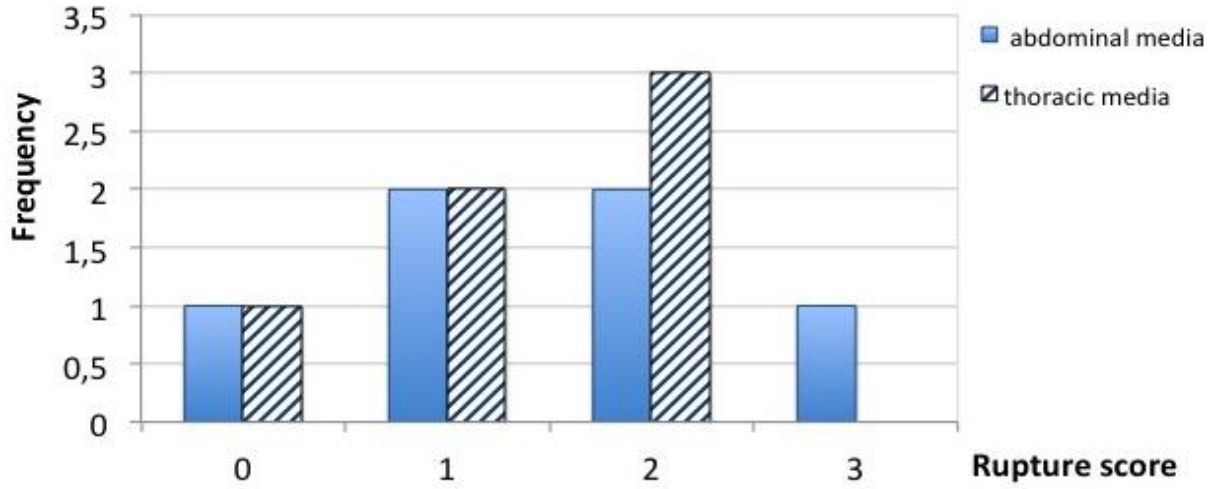

Fig.14 Similar frequency of media rupture (according to rupture score) in the abdominal and thoracic aorta after stent graft implantation.

5.10 Inflammatory CD3+ lymphocyte response- predominantly parietal

The microscopic analysis of the CD3+ cell count showed a prominent infiltration of the parietal part of the neointima.

Table 6 CD3+ positive T-lymphocyte count

Sheep	*Stent graft Position*	*CD3 luminal*	*CD3 parietal*	*Stent graft Position*	*CD3 luminal*	*CD3 parietal*
1	Abdominal	1	24	Thoracic	6	26
2	Abdominal	1	9	Thoracic	1	5
3	Abdominal	3	22	Thoracic	2	21
4	Abdominal	4	10	Thoracic	1	5
5	Abdominal	23	35	Thoracic	4	34
6	Abdominal	1	11	Thoracic	5	9
Mean (SD)		5,5 (± 7.9)	18,5 (± 9.4)		3.2 (± 2)	16.7 (±11.1)

Number of counted CD3+ T-Lymphocytes, mean and standard deviation (SD)

The interindividual difference in the CD3 + infiltration was remarkable (Table 6), but there was no statistically significant difference between the position of the stent graft in

the thoracic or abdominal part of the aorta. The CD3+ cells were also irregularly distributed in the neointima.

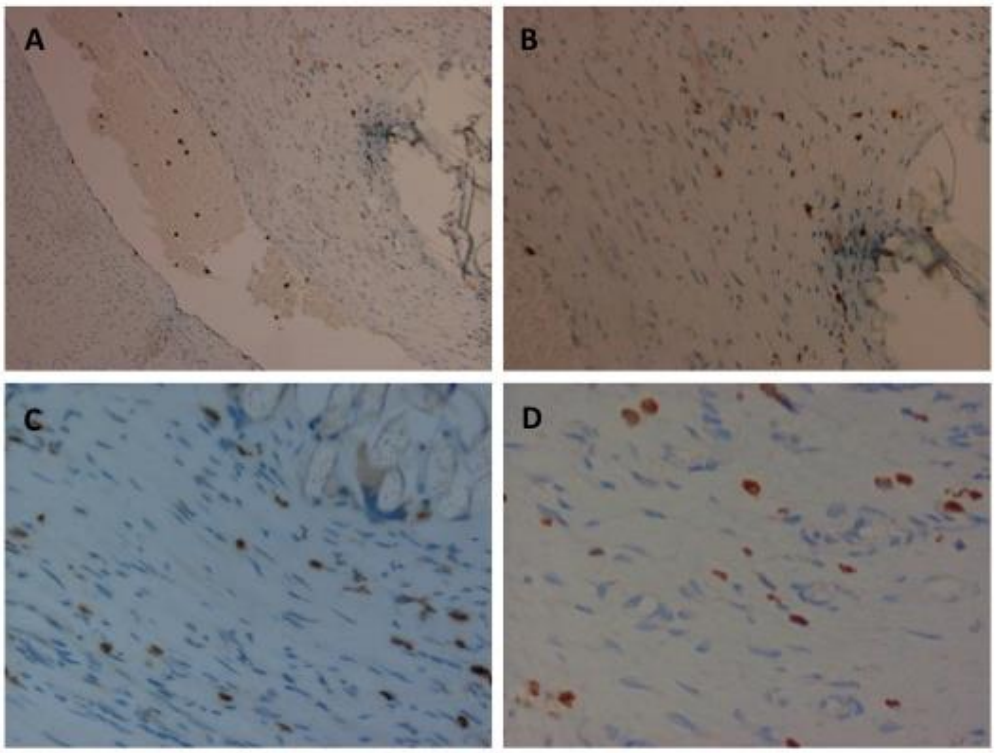

Fig. 15 Irregularly distributed CD3-positive T-lymphocytes infiltrate the tissue around the stent graft. Staining with a polyclonal Anti-CD3 antibody (brown), nucleus counterstain (blue) pictured stains of the neointima at 40x magnification (A,B) and 100x magnification (C, D).

5.11 Angiogenesis correlates with neointima hyperplasia, media atrophy and rupture

The quantitative analysis of 2 regions of interest (ROI) on WHPS stained slides of Part 2 (Fig. 5) found angiogenesis prominently in the parietal part of the neointima, with the number ranging from 1 to 31 vessels per High power field (HPF). On average, 12.2 (± 9.9) neo-vessels were found per counted HPF in the abdominal and 5.8 (±5.0) thoracic sample.

There was no statistically significant difference between the number of vessels in the abdominal and thoracic samples but again a high interindividual difference was found.

Table 7 Neovascularization

Sheep	*Position*	*Counted vessels*	*Position*	*Counted vessels*
1	Abdominal	15	Thoracic	5
2	Abdominal	5	Thoracic	10
3	Abdominal	6	Thoracic	15
4	Abdominal	1	Thoracic	2
5	Abdominal	15	Thoracic	1
6	Abdominal	31	Thoracic	2
Mean		12.2 (± 9.9)		5.8 (±5.0)

Mean number of counted vessels per HPF in each sample (± SD

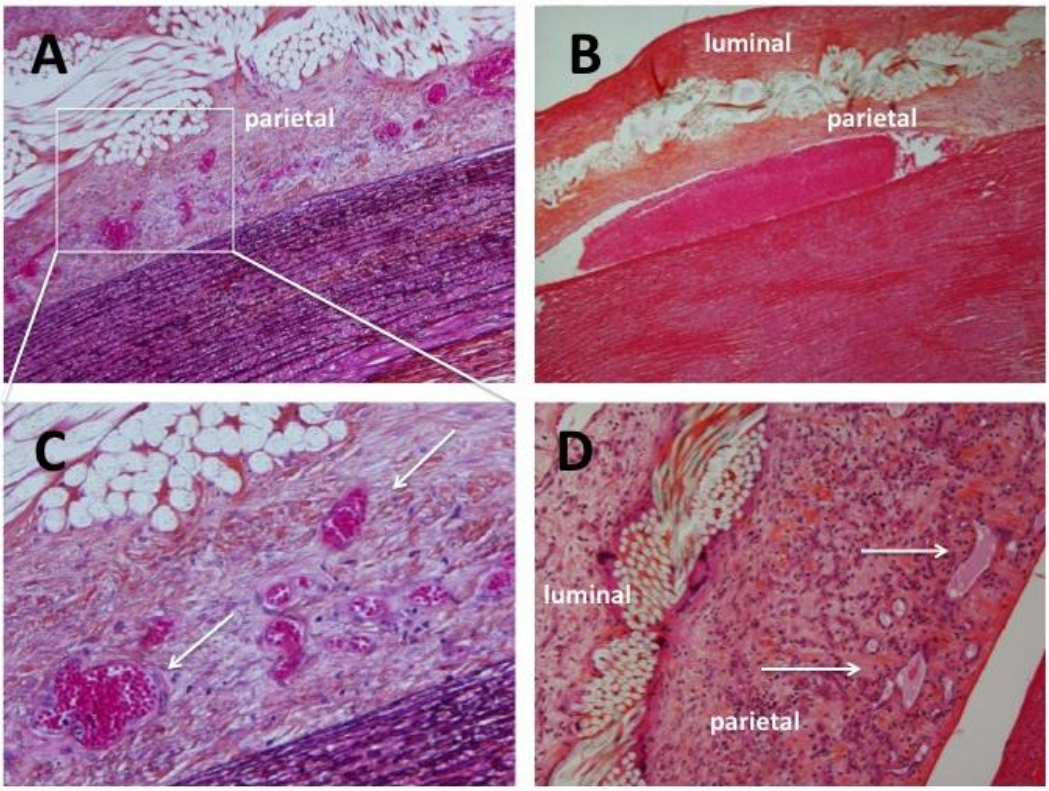

Fig. 16 Angiogenesis and dense fibrous extra-cellular matrix in the neointima

A, C WHPS stained sections; B, D HES staining; white arrows= angiogenesis; A, B shown at 40x magnification, inlets C and D shown at 100x magnification.

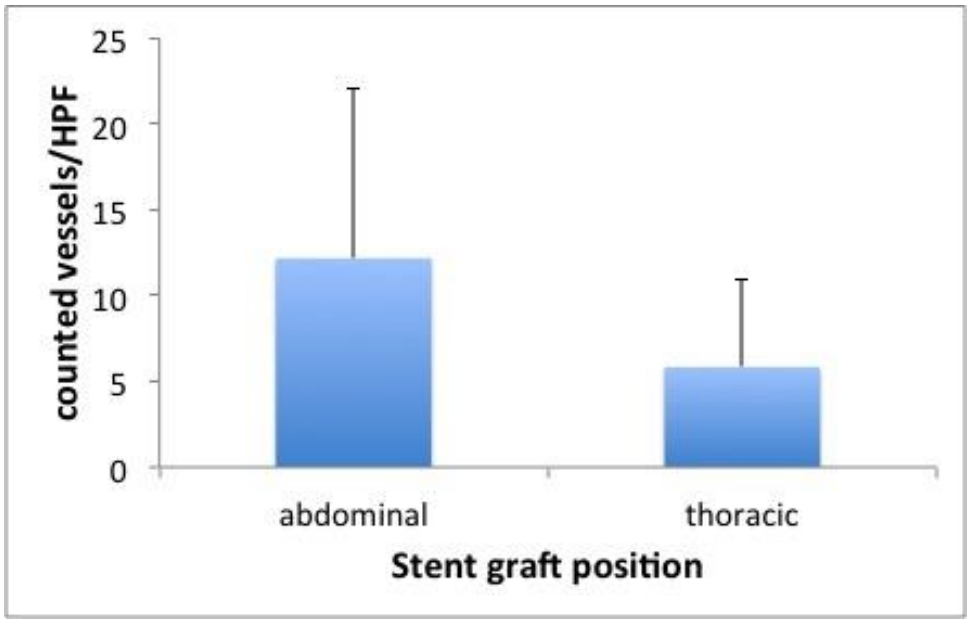

Fig. 17 Angiogenesis in abdominal and thoracic samples

The mean number of vessels counted per HPF was 12.2 （± 9.9) in abdominal and 5.8 （± 5.0) in the thoracic samples; () SD, T error bars, difference were not significant (p>0,05)

With the high interindividual differences in angiogenesis and CD3+ inflammatory reaction, the following analysis tried to identify factors that determine this individual reaction pattern, which might explaining these findings.

Table 8 Relationship between different variables

Testvariable	Rupture score	CD3+ cell count	Angiogenesis
Stent diameter	0,066	0,11	0,046
Intima thickness	0,194	0,073	0,355
Neointima thickness	0,44	0,058	0,208
not-stented media thickness	0,0001	0,0013	0,105
media atrophy	0,531	0,023	0,256
Angiogenesis	0,208	0,004	1
CD3 Cellcount	0,126	1	0,2
Rupture score	1	0,12	0,004

Values represent squared correlation coefficients (=R^2) based on a linear trend regression analysis model, with R^2 = 1 total correlation; R^2 =0 no correlation.

At first, the relationship between angiogenesis and changes in vessel wall diameters were examined (Fig. 18).
Indeed, a trend towards a correlation between angiogenesis and the neointima hyperplasia (Fig 18 C) and media atrophy (Fig. 18 D) was found when correlation coefficients were calculated for the different available variables based on a linear regression model. There was a negative correlation of the untreated vessel wall thickness with the number of angiogenic vessels in the stent tissue (Fig. 18 A+B) but a positive relation between neointima hyperplasia (Fig.18 C) and a negative media atrophy (Fig. 18 D). However, a fine differentiation of what is the cause and what are only related findings or an epiphenomenon of the observed angiogenesis, neointima hyperplasia and inflammation need a different design of the study and will be addressed in further studies.

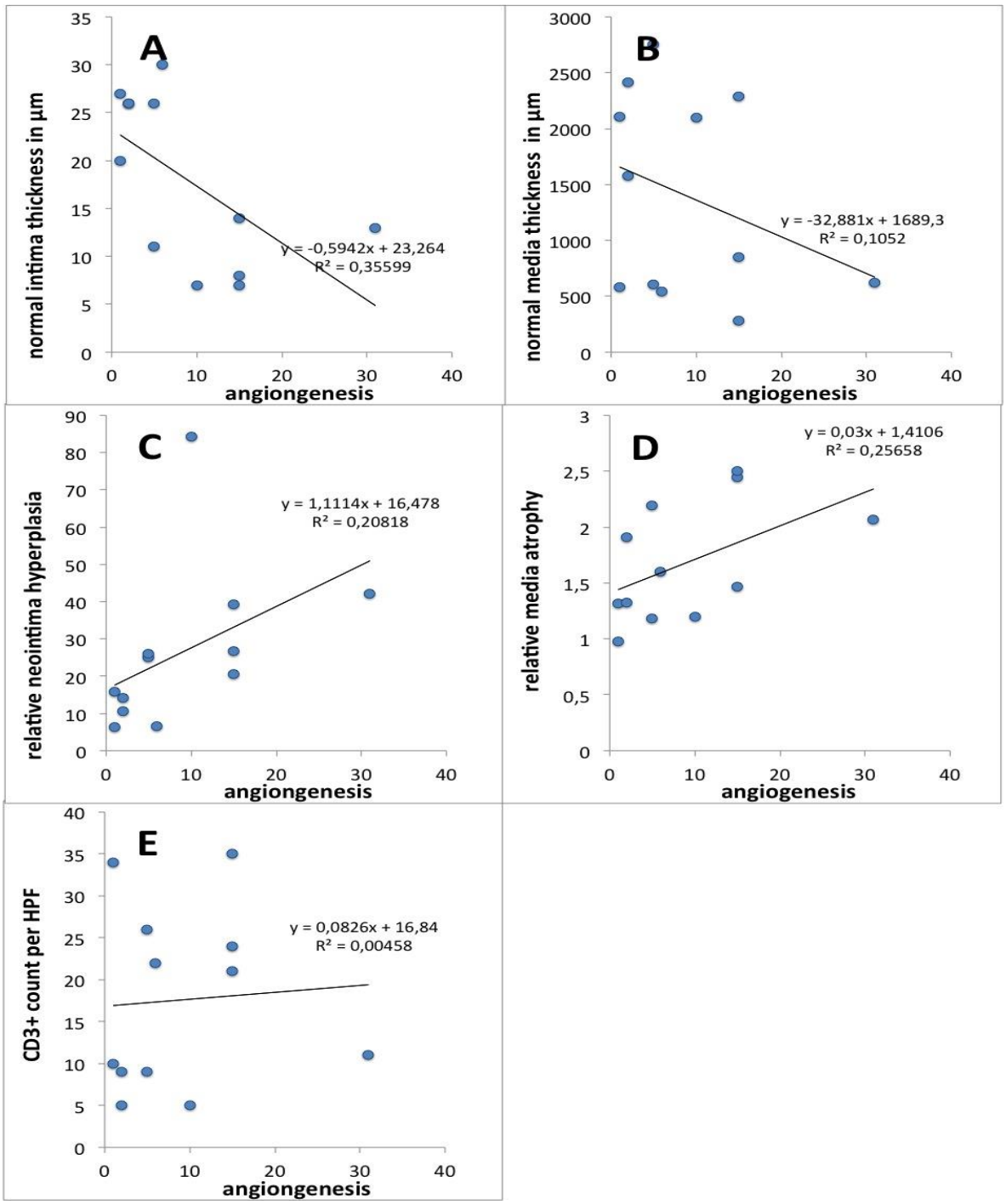

Fig. 18 Relationship between angiogenesis and vessel thickness of the non-stented and stented aorta. The number of angiogenic vessels shows a negative correlation with the normal intima thickness (A) and the normal media thickness (B) measured in the non-stented aorta. Angiogenesis correlates positively with relative neointima hyperplasia (C), negatively with relative media atrophy (D) and not with CD3+ T-lymphocyte infiltration. Scatterplot with linear trend based on minimal squares, with R^2 = 1 total correlation; R^2 =0 no correlation.

Since some published studies suggested a correlation between the stent diameter and rupture or angiogenesis, the trend analysis was used to test this hypothesis. However

there was no trend or correlation found between stent diameter and the risk of rupture or angiogenic changes in the neointima and media (Fig. 19) with the R^2 below 0.01.

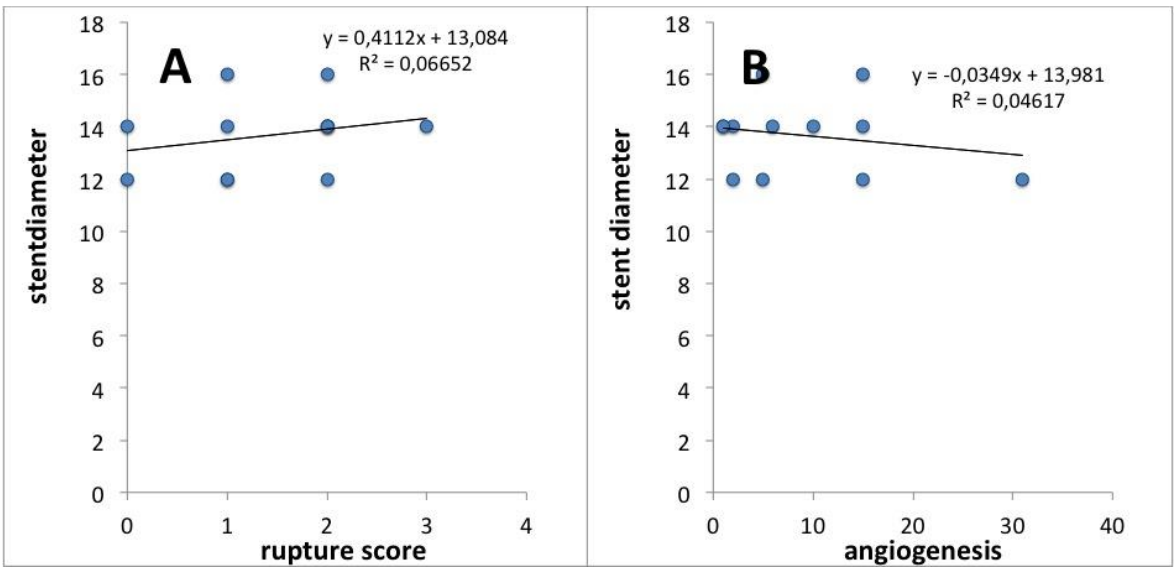

Fig. 19 The stent diameter shows no correlation with (A) the risk of rupture or (B) the angiogenesis (number of vessels) with R^2 <0.1. Scatterplot with a linear trend based on minimal squares, with R^2 = 1 total correlation; R^2 =0 no correlation.

5.12 Rupture score correlates positively with media atrophy and CD3+ infiltration but negatively with neointima hypoplasia and angiogenesis

One central question addressed was whether relative neointima hyperplasia correlates with media rupture, and wether angiogenesis and CD3+ inflammation correlate with vessel rupture. A negative correlation was found between the relative neointima hyperplasia (Fig. 20A) and the rupture score but a positive correlation between the relative media atrophy and the risk of rupture (Fig. 20B) as indicated by the rupture score. Therefore, increased rupture seems to be related with increased media atrophy, but not with baseline media thickness. Also a small positive correlation between the rupture score and CD3+ inflammatory infiltration was seen (Fig.20D).

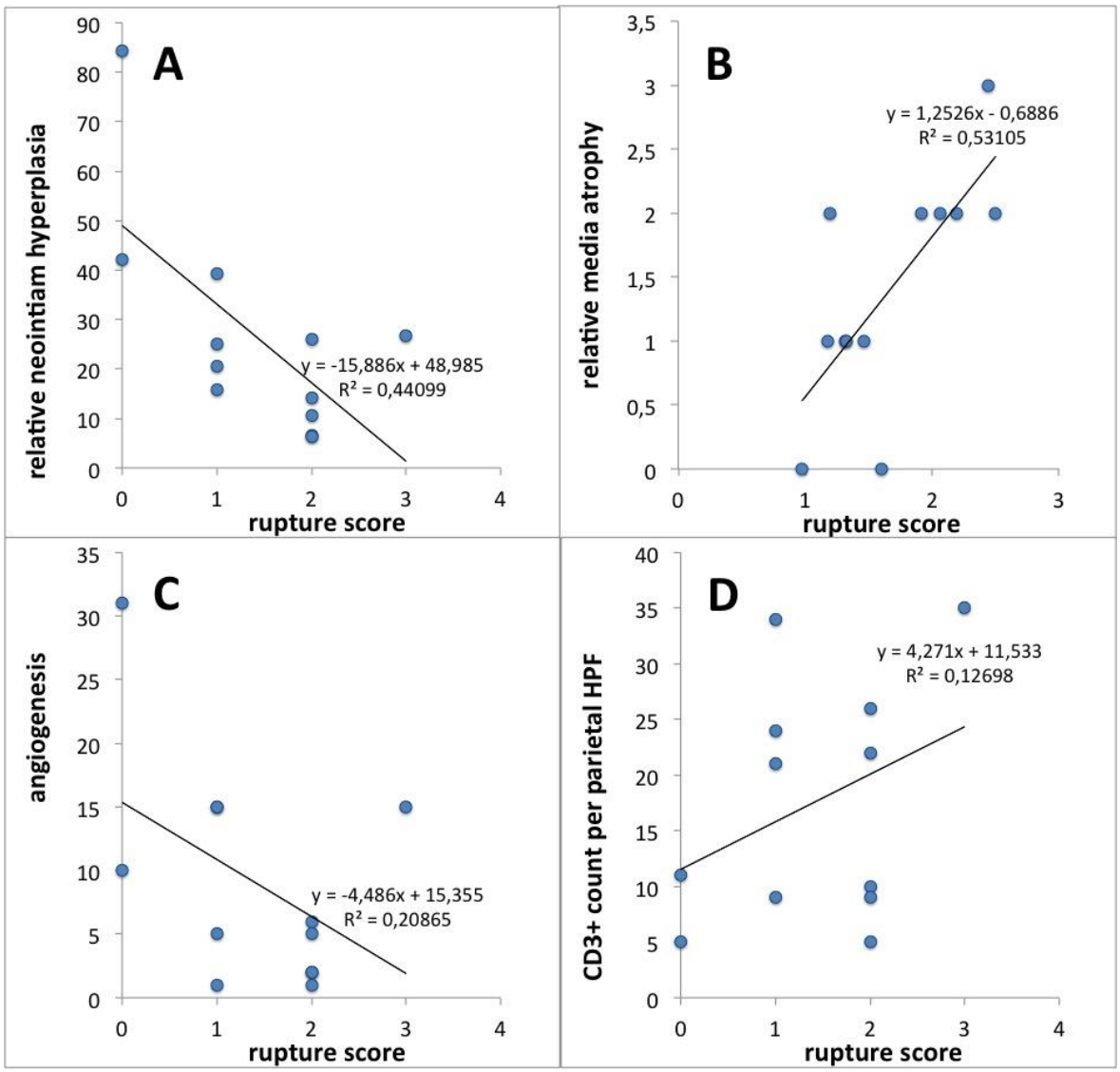

Fig. 20 Rupture score shows a negative correlation between the relative neointima hyperplasia (A) and angiongenesis (C) but a positive correlation between the relative media atrophy (B) and CD3+ count per HPF (D) Relative neointima hyperplasia=neointima thickness/intima thickness; relative media atrophy= media thickness non-stented aorta/ media thickness stented aorta. Scatterplot with a linear trend based on minimal squares, with R^2 = 1 total correlation; R^2 =0 no correlation.

5.13 CD3+ infiltrates correlate with rupture score

Also CD3+ T-lymphocyte staining in sections after long-term stent placement was used as a general marker of chronic inflammation. An ongoing chronic inflammation would explain worse outcome depending on type and material of the stent, and could be an explanation for the extensive fibroblast proliferation and increased angiogenesis. Consistent with this hypothesis, a clear trend towards increased rupture with higher CD3 counts in the sections (Fig. 20 D) was seen. But this study found no correlation

between the CD3+ counts and angiogenesis (Fig.18 E). There was no correlation or clear trend between CD3+ infiltration and media thickness or atrophy (Fig. 21 B+D). Furthermore, CD3+ cell number showed only a minimal (negative) correlation with the thickness of the normal intima and the neointima hyperplasia (Fig. 21 A+C).

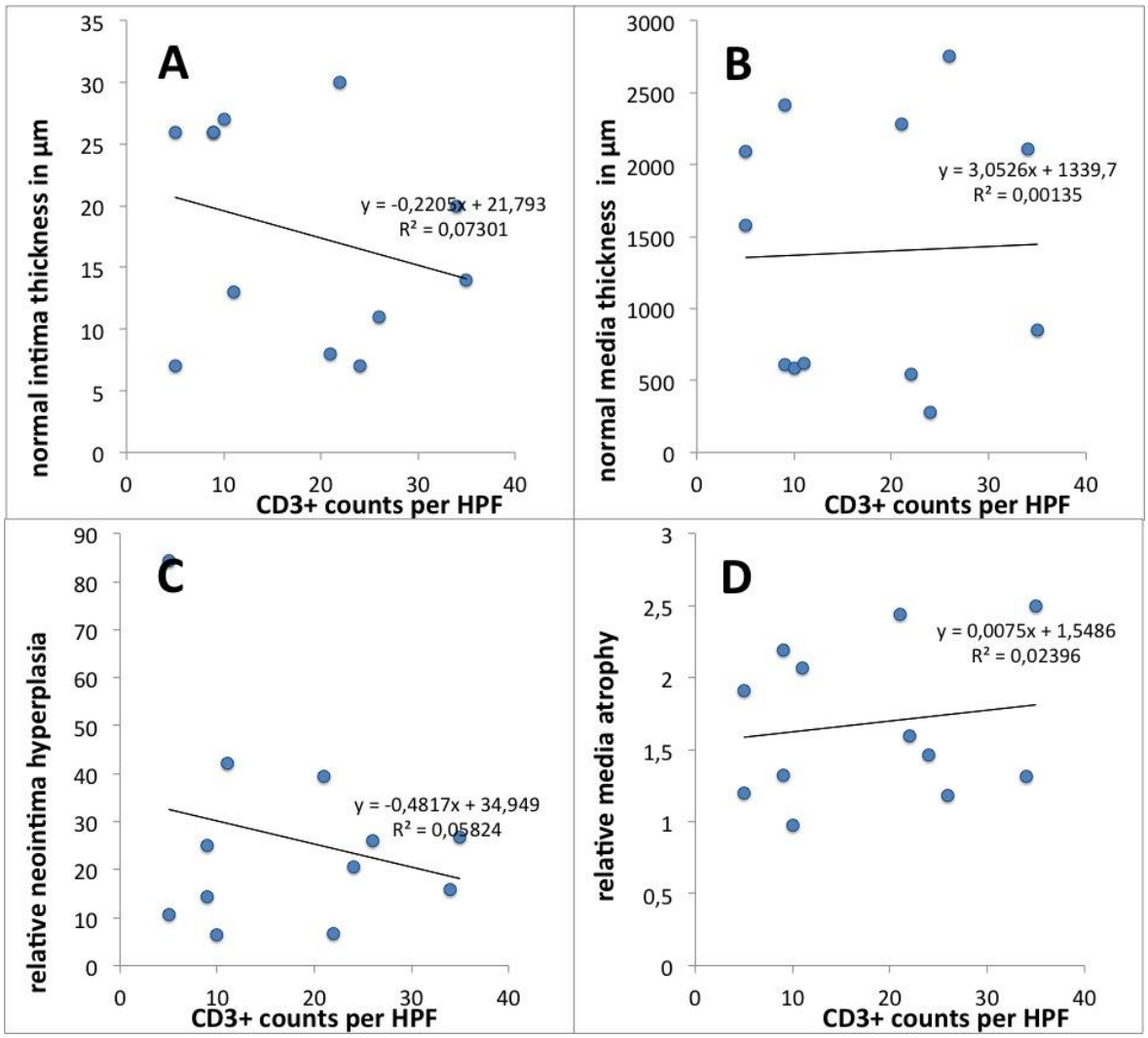

Fig. 21 CD3+ inflammatory infiltration shows only a slight negative correlation with intima thickness and neointima hyperplasia and does not correlate with media thickness or media atrophy. Scatterplot with a linear trend based on minimal squares, with $R^2 = 1$ total correlation; $R^2 = 0$ no correlation.

5.14 Chronic inflammation is visibly by foreign body reaction

As chronic inflammation and reaction to non-biocompatible material are clear causes of fibrosis and angiogenesis as described in the introduction, sections of the explanted stents were also screened for granulomas. Remarkably, the whole surface of the stents was covered with multinucleated, epitheloid like granulomas with basophilic cytoplasm

(Figs. 22 and 23). This was easily visible even at low magnification, while depending on the individual animal, the extent and the type of these granulomas varied.

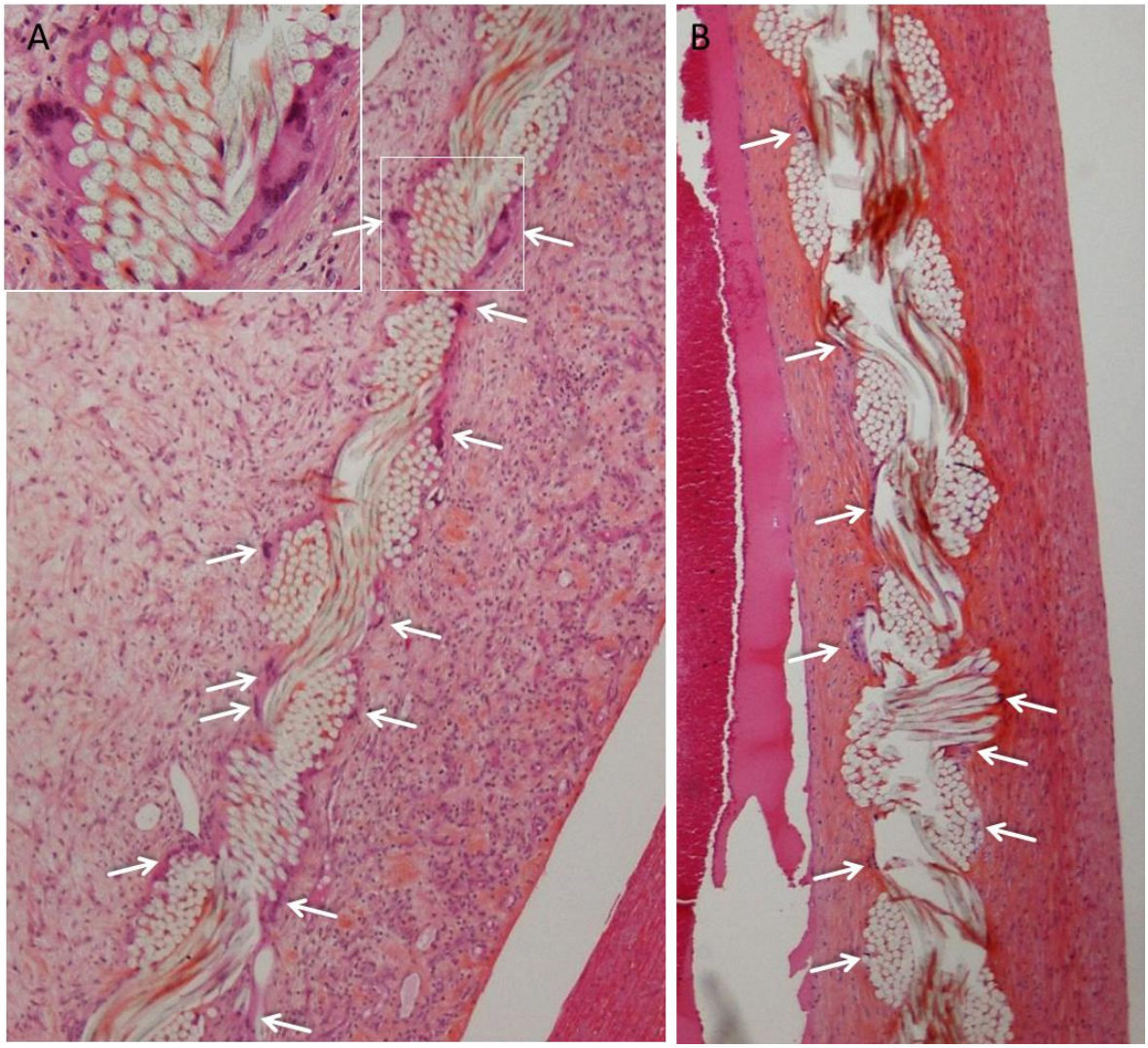

Fig. 22 Multinucleated foreign body giant cell granulomas are visible on the whole surface of explanted stents (FBGC and LGC: white arrows in two representative slides.)

Commonly observed were small sized Langhans-type giant cells in which single fibers of the stent were surrounded by an epitheloid cell syncytium, with only a few nuclei (around 2-5) being visible (Fig. 23A granuloma on the left side surrounding one fiber and Fig. 23C). In addition, directly at or a few micrometers distant from the stent, larger granulomas with dozens of nuclei representing typically Foreign-body-type giant cells were visible (Fig. 23A granuloma on the right side, Fig. 23B, D and E).

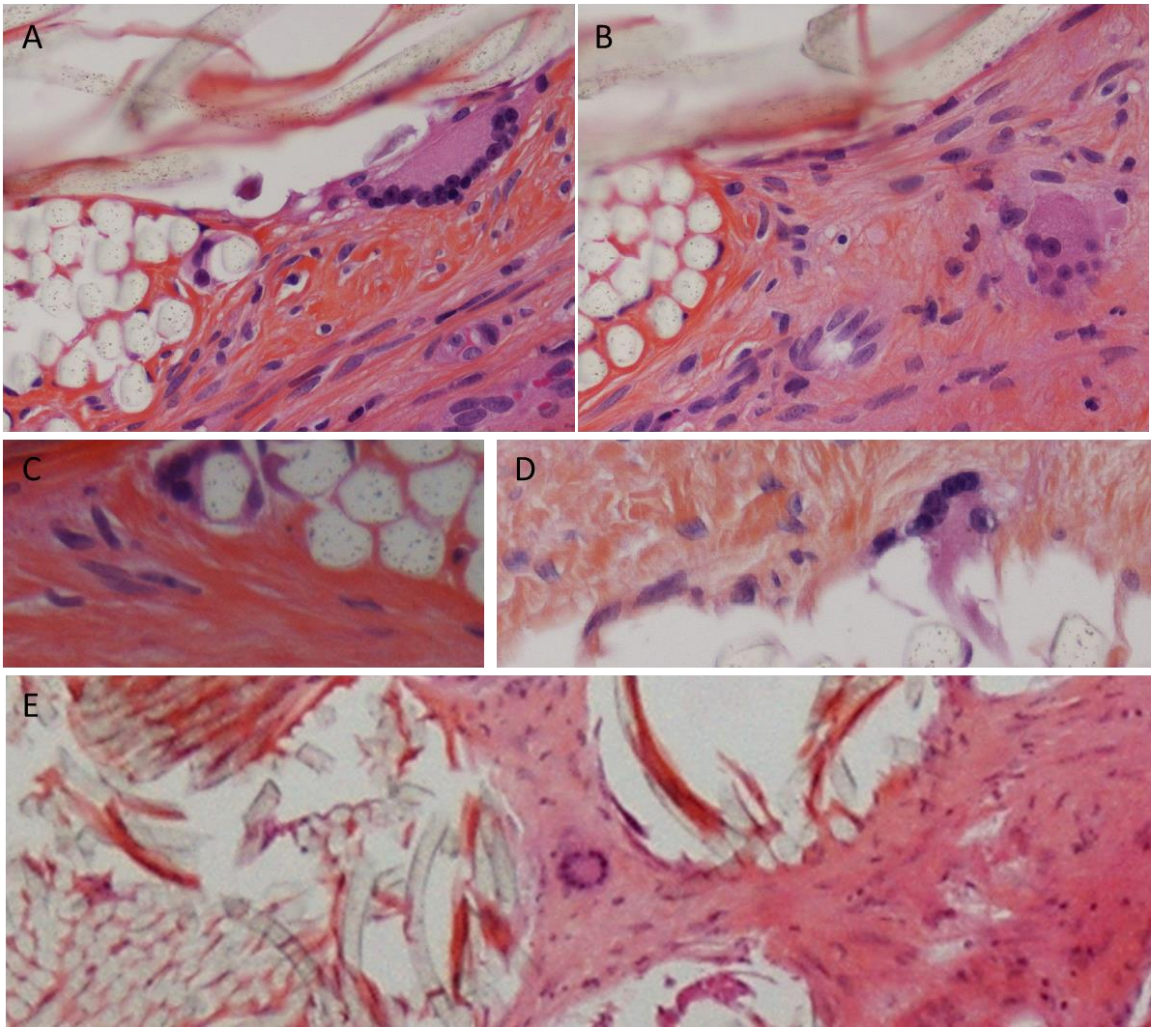

Fig. 23 Different types of multinucleated giant cell granulomas can be seen. LGC in slide A, E; FBGC in B,C, D

Many organizing MGN were visible, some forming middle-sized primary granulomas. Most of the large granulomas were secondary granulomas of the foreign body type without any visible asteroid body or any Schaumann bodies clearly excluding sarcoid-type granulomas (Fig. 23). No fibrinoid necrosis was visible, however Langhans giant cells were often found next to the stent material. The observed granulomas were therefore, predominantly foreign body type granulomas, the presence of Langhans-cells suggested the formation of tuberculosis-type granulomas in the neointima.

6 Discussion

6.1 Study Design

The study was designed to assess and evaluate the safety, biocompatibility and toxicity of L 605 chrome-cobalt stent grafts at 6-months implantation in an animal model. In particular the neointima formation and vessel wall reaction to the stent graft were analyzed.

The benefits of the investigation lie in the long-term investigation of six month which is a longer period of time than in most of the experimental studies with a comparable setup that are usually limited to a 3-month period (Schurmann, Vorwerk et al. 1997, Cejna, Virmani et al. 2001, Cejna, Virmani et al. 2002, Yavuz, Geyik et al. 2006).

The duration of six months was defined by the French authorities in the guidelines for the testing of aortic stent grafts (AFSSAP and DEDIM 2001). The novelty of the investigation and the results could have been enhanced by a direct comparison with a group of sheep carrying another stent graft material (e.g. 316 stainless steel). However, the experiment was based on earlier studies in the same setting at the Institute of Vascular Implants (Koskas, Cluzel et al. 1999, Koskas, Brocheriou et al. 2005, Oberhuber, Buecken et al. 2012) and given the fact that the chrome-cobalt L 605 has been used in other studies before, it was decided against a direct control group. At this early stage of the Clearpass project scientific rigor had to be weighted against the ethical arguments of testing animals repeatedly with the same material.

Also, the study question focused on safety issues associated with the employment of this particular stent material with the established methods for CMSG at the Institute of Vascular Implants. The question was not whether stents made of 316 stainless steel, tungsten chrome cobalt L 605 or nitinol were better. This question has already been addressed in different animal studies in the past (Schurmann, Vorwerk et al. 1997, Cejna, Virmani et al. 2002). Given the limits of any animal model, the real advantage and direct comparison of the stent material for the different categories established in this experiment (neointima building, wall reaction etc.) will eventually have to be proven in human patients rather than sheep.

6.2 Animal Model

There are two different types of animal models mainly used to study the therapy of aortic aneurysm: The large animal models such as pigs (Siegenthaler, Celik et al.

2008), sheep (Ueberrueck, Tautenhahn et al. 2005) and dogs (Barth, Virmani et al. 1996, Bashar, Kazui et al. 2002) are mostly used to study the surgical repair of aortic aneurysm (Bashar, Kazui et al. 2002, Molacek, Treska et al. 2009), while the smaller animal models such as mice and rats are used to study the underlying disease mechanisms by artificially creating specific metabolic circumstances leading to aortic aneurysm (Merino, Todiras et al. 2009, Trollope, Moxon et al. 2011).
The elastase-induced aneurysm model for pigs (Molacek, Treska et al. 2009) or the angiotensin II-induced apoE $^{-/-}$ Knockout mice ((Merino, Todiras et al. 2009) and the *in vitro* bovine models (Bosman, Steenhoven et al. 2010) are between these two groups, but these models were unavailable for the current study.

Among the large animal models, the sheep is an established animal model used in vascular surgery. According to a study comparing the use of pigs and sheep as animal models, both produce comparable results (Ueberrueck, Tautenhahn et al. 2005). The advantage of the sheep model is that their coagulation system is closer to that of the human species whilst at the same time being more stress resistant (Ueberrueck, Tautenhahn et al. 2005).
The main disadvantage of the sheep used in this study was that they were healthy and therefore did not provide the typical endothelial pathologies, associated withthe vessel dilatation, aneurysm and difficult endothelial healing that surgeons usually face in patients with aortic aneurysm. Also being non-congenic a high intra-individual difference in response to implantation was observed in our model.
Patients undergoing EVAR are usually under life-long treatment with aspirin or other antiaggregation medications designed to inhibit the development of a thrombotic event at the luminal surface of the stent graft. But the animals were not receiving any baseline anticoagulative medication. This explains the complete neointima covering, which could not be expected in human patients (Elkouri, Gloviczki et al. 2004) and which even surpassed the neointima formation observed in other studies (Ueberrueck, Tautenhahn et al. 2005).

6.3 Stent grafts

The stent graft production was technically successful in all cases. The twelve stent grafts explanted from the sheep remained macroscopically intact after 6 months of implantation, but clearly the diameter chosen was too large to fit into the native aorta in the abdominal samples (van Prehn, Schlosser et al. 2009). The problem with the current stent graft production lies in the fact that the 18F introducer system is the smallest approved for the CMSG produced in the Institute of Vascular Implants. It is therefore impossible to produce smaller stent grafts without changing the whole introducing system necessitating a new approval procedure.

6.4 Implantation

The main difficulties during the implantation were encountered while pushing the stent-grafts upwards because the small vessel diameter in the sheep did not allow for a safe navigation with an 18Fr introducer system and led to tearing of the intima in three cases. The same problem was encountered in a previous study in 2005 at the Institute of Vascular Implants.
To date no alternative, bigger animal model exists for studying the safety and biocompatibility of customized stent grafts at the Laboratory of Vascular Implants, Hôpital Pitié-Salpêtrière. The problem of the introducer system is unique to the CMSG developed at this laboratory.

To avoid the loss of 30% of the test animals in future studies it is recommended to anastomose a prosthetic carrier graft to the native aorta, through which the stent-graft and the introducer system could be introduced into the native aorta, since smaller introducers will make the use of the metallic cone to load the introducer system impossible.
„In our clinical experience [...] the range of the maximal transverse diameter of stent-grafts used for aortic aneurysm repair in humans is 12 to 44 mm. This range corresponds to a range of appropriate introducers with a diameter of 18 to 24 F. [...] For the deployment of stent-grafts of these diameters among humans, the use of introducers of 18 Fr. is mechanically satisfactory and allows navigation from a femoral access in nearly all cases.“ (Koskas, Brocheriou et al. 2005)

6.5 Explantation

The explantation of the 12 stent grafts was technically successful in all 6 sheep and allowed for a systematic evaluation of the stent grafts in the beating aorta *in situ*. It would have been desirable to take blood samples for inflammatory markers (CRP, leucocytes etc.) to control any possible inflammatory process due to the stent graft. But due to the fact that the sheep were only brought to the stables of the operation site on the day of the explantation, it was impossible to establish a baseline value and/ or detect any possible confounders. Given that the primary interest of the study was to assess the long-term interactions between the stent graft and aorta and given the fact that every explant was systematically and extensively analyzed microscopically for any signs of bacterial infection, the exclusion of additional laboratory workup to detect any ongoing bacterial infection is acceptable.

6.6 Radiological Analysis

The radiological analysis showed no migration or leakage from any of the implanted stent grafts. All adjacent vessels were patent after six month of implantation. There were no visible thrombi or stenoses. However some of the implanted stent grafts were clearly oversized on fluoroscopy. Compared to the isometric analysis, the mismatch seemed less prominent on the radiological planes, this was also reported by other groups (Siegenthaler, Celik et al. 2008). This is due to the fact that measurements were taken after the vessels had been processed for microscopic evaluation in buffered formalin, leading to loss of elasticity and volume depletion of tissue. Our results confirm the experimental results of CMSG using a stainless steel alloy (Koskas, Brocheriou et al. 2005).

6.7 Macroscopic safety parameters

The macroscopic safety parameters evaluated showed favorable results, notably the absence of thrombi, stenoses, aneurysms and endoleakage. The stent grafts served as patent aortic substitutes during six month implantation. This study confirms the results from an earlier study testing CMSG in sheep using a stainless steel alloy (Koskas, Brocheriou et al. 2005).

In some implanted stent grafts infolding was observed. In the literature infolding is reported to occur with oversized stent grafts > 30% vessel diameter with an adverse thoracic angulation in humans (van Prehn, Schlosser et al. 2009, Kasirajan, Dake et al. 2012). On the other hand *in vitro* experiments show that the best apposition for abdominal aortic stent grafts is achieved with 30% only (Mestres, Uribe et al. 2012). In clinical practice the CMSG production aims at the recommended oversizing of 10-20% (Koskas, Brocheriou et al. 2005, van Prehn, Schlosser et al. 2009).

6.8 Neointima hyperplasia and media atrophy

In this study the observed neointima thickness and media atrophy were compared to the intima and media thickness measured in the proximal and distal non-stented sections of the aorta. Therefore, one could argue that these measurements lack healthy aortic controls. In a comparable study in pigs in 2008 the intima, media and neointima formation was measured in a very similar manner (Siegenthaler, Celik et al. 2008). Siegenthaler, Celik et al. compared their intima and media measurements proximal and distal of the stented aorta to the aorta of stent free animals and found no difference. This makes it unlikely that the accuracy of the observed results, namely the neointima hyperplasia and the media atrophy, would have been significantly different when compared to the aorta of an entirely stent free sheep.

6.8.1 Neointima thickness

The neointima hyperplasia reported in this study is slightly higher than the one described in the literature (Ueberrueck, Tautenhahn et al. 2005). This might be due to the fact that the 6 months of endovascular implantation required by the French authorities are rarely completed in the scientific literature, where most experiments terminate after 3 months (Cejna, Virmani et al. 2002) with only one exception, where stent grafts in sheep were evaluated after 1 year in sheep (White, Mulligan et al. 1998). This group also found an incorporation of the stent graft with neointima formation showing smooth muscle cells and collagen content.

6.8.2 Media atrophy

The results of this study regarding reduced media thickness in oversized stents confirm that whilst a mild (10-20%) oversizing of the stent graft is desirable for the secure anchoring, a further increase can lead to a significant media loss and adverse effects as observed by other groups (White, Mulligan et al. 1998, van Prehn, Schlosser et al. 2009).

The interpretation of these results is that further systematic research in this field is needed. The observed adverse effects of media atrophy strongly show the need for custom made stent graft aimed at optimal individualized fit that was regrettably unavailable for the test animals.

6.9 Semiquantitative score for media rupture

Many studies on stent-related vascular reactions focus mainly on neointima hyperplasia probably in the tradition of coronary stent analysis. Nonetheless, media rupture has been observed by several other studies in sheep (White, Mulligan et al. 1998, Bashar, Kazui et al. 2002) and pigs (Scheumann, Heilmann et al. 2012).
These studies all describe the impact of the radial stent force on the thickness and undulation of medial lamellar units (MLU) and “focal replacement by collagen of the inner one third to one half of the media at the proximal anchor sites “(White, Mulligan et al. 1998).
Bashar introduced in 2002 the count of MLU as an analytic tool to quantify the media atrophy (Bashar, Kazui et al. 2002).
For this study this concept was extended to include the qualitative changes in MLU arrangement in a semiquantitative score of media rupture. Therefore the presented findings regarding the media changes after long-term stent placement represent new data confirming a general, time-dependent and ongoing media atrophy associated with stent therapy that can also happen in patients (Major, Guidoin et al. 2006, Kasirajan, Dake et al. 2012).

6.10 Inflammatory CD3+ lymphocyte response - predominantly parietal

The predominantly parietal infiltration of CD3+ T-lymphocytes found in this analysis confirms earlier findings (Ueberrueck, Tautenhahn et al. 2005). The infiltration of the

vessel wall with T-lymphocytes is associated with the chronic, granulation phase of foreign body reactions (McNally and Anderson 2011) that has been linked to the formation of FBGC, angiogenesis and neointima hyperplasia.

6.11 Angiogenesis correlates with neointima hyperplasia/media atrophy and vascular injury

As described above, the neointima thickness is largely based on extensive fibrosis with only a minimal increase in the endothelial cell layer. As fibroblasts similar to endothelial stem cells leading to angiogenesis are the typical cell type found during scar formation in large blood vessels together with various immune cells, this study tried to identify whether both might be stimulated by the stent graft implantation. The results showed a trend for a correlation between the neointima hyperplasia and angiogenesis. The dependent relationship between angiogenesis and neointimal hyperplasia has been shown in at least three other models (mice and rats) (Khurana, Zhuang et al. 2004) and pigs (Izzat, Mehta et al. 1996). The presented results therefore represent new data on this phenomenon in the sheep aorta after stent graft implantation.

However due to the unexpectedly high variance of the angiogenesis and CD3+ infiltration, the results presented here are only trends for correlation and do not necessarily present a causal relationship. This has to be addressed in further studies.

Interestingly, it was found that some animals with thinner vessel walls in the non-stented aorta (both media and intima) responded with a higher rate of angiogenesis to the stent grafting. These animals also showed a higher neointima hyperplasia and stronger media atrophy after stent graft implantation (Fig. 21 C+D). This might demonstrate the important influence of genetic and developmental factors on the inflammatory response in every individual after stent grafting, which has also been observed in humans (Kim, Ko et al. 2012). Since there are currently no known biomarkers predicting a strong inflammatory response it is difficult to identify and medically target this subset of patients.

6.12 Rupture scores correlate with media atrophy

The trend for a positive correlation of the rupture score with the relative media atrophy but not the neointima hyperplasia shows that the rupture score is a specific tool to semiquantitatively detect mechanical injury after stent graft implantation. This has also

been observed in other studies especially in the thoracic part of the aorta (Scheumann, Heilmann et al. 2012). However these trends are only preliminary findings and the validity of this new tool for assessing media injury will have to be tested in future studies.

6.13 CD3+ infiltrates correlate with rupture score

Some authors (Anderson, Rodriguez et al. 2008) suggest that the infiltration with T-lymphocytes in the chronic phase of foreign body reactions is predominantly of a T_H2 (IL-4, Il-13) cytokine pattern, aimed at a suppression of the local foreign body reaction. The cell count of CD3+ cells is a pan-T-Cell staining unfit to distinguish the T_H2 subset of T-lymphocytes so any comment regarding their existence in the examined specimens remains speculation. However the weak correlation of the CD3+ count with the rupture score but not any of the other pro-inflammatory markers (angiogenesis, neointimal hyperplasia, media atrophy etc.) and the presence of multiple FBGC that are known to react with these T-lymphocytes (McNally and Anderson 2011) indicate that the CD3+ cells counted in this study might function in this way in the analyzed samples. It would be very interesting to confirm this hypothesis in further studies.

6.14 Chronic inflammation is visible by foreign body reaction and might play a role in stent graft failure

In addition to the neointima hyperplasia, angiogenesis and CD3+ cell infiltration this study found evidence of a complete chronic foreign body reaction with FBGCs that is congruent with published data (Hagerty, Salzmann et al. 2000). The current study as well as the published data observed the close proximity of the chronic inflammatory reaction to the prosthetic material.

In addition to the published data a large number of Langhans-type giant cells was found in close proximity to the graft fibers. The amount of visible chronic foreign body reaction in the sample sections and especially the different types of giant cells including tuberculosis type LGC, were a surprise since they are not reported to this extent in the literature (Barth, Virmani et al. 1996, Cejna, Virmani et al. 2001, Koskas, Brocheriou et al. 2005).

It is not clear at this point whether this observation is stent specific, and whether it represents e.g. a delayed hypersensitivity reaction of the sheep aorta to the stent material, since LGC infiltration has been linked to delayed hypersensitivity reactions in the past (Knolle 1988).

On the other hand, the coexistence of several different multinucleated giant cells could also be an overlap of several giant cell types that has been described also in microscopic sections of other diseases such as sarcoidosis (Okamoto, Mizuno et al. 2003).
There seems to be some scientific dispute regarding the differences between the different types of multinucleated giant cells beyond morphology. LGCs and FBGCs are both generated from blood-derived monocytes probably via macrophage fusion (Most, Spotl et al. 1997) and they represent a lot of similar markers but it is currently unclear if FBGC and LGC have different functions (Okamoto, Mizuno et al. 2003).
As mentioned in the introduction, some authors report that *in vitro* FBGCs are induced by IL-4 and MMP-9 (MacLauchlan, Skokos et al. 2009, McNally and Anderson 2011) and that INF-gamma preferably induces LGCs (McNally and Anderson 1995).
There is however a large number of publications linking the existence and close proximity of the MGCs to the surface of implants to the degradation of materials (Anderson, Rodriguez et al. 2008) through production of reactive oxygen species (Jones, Chang et al. 2007).
The constant presence of MGCs even 6 months after implantation that are presented here, provide evidence for a potential role of these cells in late graft failures that are reported years after initial EVAR in the literature with a frequency of 0.7% to 3.3% (Harris, Vallabhaneni et al. 2000, Major, Guidoin et al. 2006, Geisbusch, Schumacher et al. 2007, Forbes, Harrington et al. 2012, Jayia, Constantinou et al. 2013).

Also a review of the literature of foreign body reactions in biomaterial studies as well as the recent publications on the inflammatory pathogenesis of aortic aneurysm (Golledge, Muller et al. 2006) showed remarkable similarities regarding the histological and molecular findings: angiogenesis, lymphocyte infiltration and ECM remodeling enzymes such as MMP 1, 3, 9, TIMP1 and TIMP2 (Jones, McNally et al. 2008, MacLauchlan, Skokos et al. 2009, Reeps, Pelisek et al. 2009), reactive oxygen species (Anderson, Rodriguez et al. 2008, Satoh, Nigro et al. 2009) and cytokine profiles (e.g. IL-1beta, IL-6, TNF-alpha; IL-4) (Swedenborg, Mayranpaa et al. 2011) (Pearce and Shively 2006, Anderson, Rodriguez et al. 2008, Schlaweck, Zimmer et al. 2011) were reported in both conditions.

These striking similarities indicate that the chronic inflammatory environment leading to aortic aneurysm might enhance stress and inflammatory reactions on the surface of the implanted stent leading to degradation of the suture material linking the graft to the stent (Anderson, Rodriguez et al. 2008) and poor vascular healing. Our histological observations, although primarily phenomenological and lacking the molecular refinement, are supported by aforementioned publications. It would be highly desirable to test this hypothesis in future experiments.

There have been various attempts to improve vascular healing through surface modifications of the stent grafts (van der Bas, Quax et al. 2004) since the first endovascular stent grafts were introduced 30 years ago. This new technique has seen a rapid and continuous improvement and it is spreading (Jayia, Constantinou et al. 2013). Today EVAR is at least equal to the former gold standard of OR in terms of numbers of interventions and it produces comparable reintervention rates (Lederle, Freischlag et al. 2012).
The latest generation of commercially produced stent grafts are based on a modular structure aiming at an optimal fit (Jayia, Constantinou et al. 2013) as customized stent grafts thereby increasing the operability and reducing the reintervention rates by securely anchoring the endovascular devices (Singland, Mitton et al. 2010).
EVAR has been very successful but some ambiguity still remains regarding especially the long term follow up of these implanted devices (Eckstein 2007). This study tried to address this in the 6-month study and the results show that the complex interactions in the aorta of healthy sheep create favorable conditions ofr inflammation and media rupture due to foreign body reaction.
In the unfavorable environment of aortic aneurysms this might lead to even worse reactions in the long- term for younger patients especially eligible for this technique (Lederle, Freischlag et al. 2012)
Realistic healing of aortic aneurysm will therefore have to include a better and more specific medical therapy of the underlying inflammatory processes (Le Manach, Ibanez Esteves et al. 2011), especially with risk factors for AA showing an increasingly global distribution pattern (e.g. the still growing number of smoking people (Giovino, Mirza et al. 2012, Thun, Carter et al. 2013) and the obesity epidemic (JC Wells 2012).
Recent basic research findings linking cyclophilin A (Satoh, Nigro et al. 2009), and the kinin B1 receptor (Merino, Todiras et al. 2009) to increased aneurysm formation in mice

via MMPS, as well as many publications investigating the role of MMPs (Reeps, Pelisek et al. 2009, Lohoefer, Reeps et al. 2012) and mast cell driven activation (Golledge and Norman 2011, Swedenborg, Mayranpaa et al. 2011) show new directions for future research aimed at optimal healing of patients suffering from aortic aneurysms.

7 Bibliography

AFSSAP and DEDIM (2001). Evaluation des endoprothèses aortiques utilisées pour le traitement endo-vasculaire des anévrismes de l'aorte abdominale sous-rénale. A. f. d. s. s. d. p. d. santé and D. D. l. e. D. D. Médicaux. ISO 7198 EN 12006-2 ISO CD 15539-1

Alicea, L. A., J. I. Aviles, I. A. López, L. E. Mulero and L. A. Sánchez. (2004). "MECHANICS BIOMATERIALS:STENTS." Applications of Engineering Mechanics in Medicine, (Assessed September 3, 2013 at http://www.pdfio.com/k-216502.html.)

Anderson, J. M. and K. M. Miller (1984). "Biomaterial biocompatibility and the macrophage." Biomaterials 5(1): 5-10.

Anderson, J. M., A. Rodriguez and D. T. Chang (2008). "Foreign body reaction to biomaterials." Semin Immunol 20(2): 86-100.

Barth, K. H., R. Virmani, J. Froelich, T. Takeda, S. V. Lossef, J. Newsome, R. Jones and D. Lindisch (1996). "Paired comparison of vascular wall reactions to Palmaz stents, Strecker tantalum stents, and Wallstents in canine iliac and femoral arteries." Circulation 93(12): 2161-2169.

Bashar, A. H., T. Kazui, H. Terada, K. Suzuki, N. Washiyama, K. Yamashita and S. Baba (2002). "Histological changes in canine aorta 1 year after stent-graft implantation: implications for the long-term stability of device anchoring zones." J Endovasc Ther 9(3): 320-332.

Biancari, F., A. Catania and V. D'Andrea (2011). "Elective endovascular vs. open repair for abdominal aortic aneurysm in patients aged 80 years and older: systematic review and meta-analysis." Eur J Vasc Endovasc Surg 42(5): 571-576.

Bosman, W. M., T. J. Steenhoven, D. R. Suarez, J. W. Hinnen, E. R. Valstar and J. F. Hamming (2010). "The proximal fixation strength of modern EVAR grafts in a short aneurysm neck. An in vitro study." Eur J Vasc Endovasc Surg 39(2): 187-192.

Cejna, M., R. Virmani, R. Jones, H. Bergmeister, C. Loewe, M. Schoder, M. Grgurin and J. Lammer (2002). "Biocompatibility and Performance of the Wallstent and the Wallgraft, Jostent, and Hemobahn Stent-Grafts in a Sheep Model." Journal of Vascular and Interventional Radiology 13(8): 823-830.

Cejna, M., R. Virmani, R. Jones, H. Bergmeister, U. Losert, Z. Xu, P. Yang, M. Schoder and J. Lammer (2001). "Biocompatibility and Performance of the Wallstent and Several Covered Stents in a Sheep Iliac Artery Model." Journal of Vascular and Interventional Radiology 12(3): 351-358.

Chaikof, E. L., D. C. Brewster, R. L. Dalman, M. S. Makaroun, K. A. Illig, G. A. Sicard, C. H. Timaran, G. R. Upchurch and F. J. Veith (2009). "The care of patients with an abdominal aortic aneurysm: The Society for Vascular Surgery practice guidelines." Journal of vascular surgery : official publication, the Society for Vascular Surgery 50(4): S2-S49.

Creager, M. A. and J. Loscalzo (2008). Disease of the Aorta. Harrison´s Principles of Internal Medicine. A. S. Fauci, E. Braunwald, D. L. Kasper et al. New York USA, Mc Graw Hill Medical II: 1563-1564.

Dugast, C., A. Gaudin and L. Toujas (1997). "Generation of multinucleated giant cells by culture of monocyte-derived macrophages with IL-4." J Leukoc Biol 61(4): 517-521.
Eckstein, H. H. (2007). "[Open vs endovascular surgery : current status]." Chirurg 78(7): 581-582.

Elkouri, S., P. Gloviczki, M. A. McKusick, J. M. Panneton, J. Andrews, T. C. Bower, A. A. Noel, W. S. Harmsen, T. L. Hoskin and K. Cherry (2004). "Perioperative complications and early outcome after endovascular and open surgical repair of abdominal aortic aneurysms." J Vasc Surg 39(3): 497-505.

EVAR-TRIAL-1 participants. (2005). "Endovascular aneurysm repair versus open repair in patients with abdominal aortic aneurysm (EVAR trial 1): randomised controlled trial." The Lancet 365(9478): 2179-2186.

EVAR-Trial-2 participants. (2005). "Endovascular aneurysm repair and outcome in patients unfit for open repair of abdominal aortic aneurysm (EVAR trial 2): randomised controlled trial." The Lancet 365(9478): 2187-2192.

Forbes, T. L., D. M. Harrington, J. R. Harris and G. DeRose (2012). "Late conversion of endovascular to open repair of abdominal aortic aneurysms." Can J Surg 55(4): 254-258.

Geisbusch, P., H. Schumacher, J. Hansmann, J. R. Allenberg and D. Bockler (2007). "Late aneurysm rupture after repressurization of a thrombosed stent-graft." J Endovasc Ther 14(5): 672-675.

Giovino, G. A., S. A. Mirza, J. M. Samet, P. C. Gupta, M. J. Jarvis, N. Bhala, R. Peto, W. Zatonski, J. Hsia, J. Morton, K. M. Palipudi and S. Asma (2012). "Tobacco use in 3 billion individuals from 16 countries: an analysis of nationally representative cross-sectional household surveys." Lancet 380(9842): 668-679.

Golledge, J., J. Muller, A. Daugherty and P. Norman (2006). "Abdominal aortic aneurysm: pathogenesis and implications for management." Arterioscler Thromb Vasc Biol 26(12): 2605-2613.

Golledge, J. and P. E. Norman (2011). "Current status of medical management for abdominal aortic aneurysm." Atherosclerosis 217(1): 57-63.

Greenberg, R. K., Q. Lu, E. E. Roselli, L. G. Svensson, M. C. Moon, A. V. Hernandez, J. Dowdall, M. Cury, C. Francis, K. Pfaff, D. G. Clair, K. Ouriel and B. W. Lytle (2008). "Contemporary analysis of descending thoracic and thoracoabdominal aneurysm repair: a comparison of endovascular and open techniques." Circulation 118(8): 808-817.

Greenhalgh, R. M., L. C. Brown, G. P. Kwong, J. T. Powell, S. G. Thompson and E. t. participants (2004). "Comparison of endovascular aneurysm repair with open repair in patients with abdominal aortic aneurysm (EVAR trial 1), 30-day operative mortality results: randomised controlled trial." Lancet 364(9437): 843-848.

Guivier-Curien, C., V. Deplano, E. Bertrand, J. Dominique Singland and F. Koskas (2009). "Analysis of blood flow behaviour in custom stent grafts." J Biomech 42(11): 1754-1761.

Hagerty, R. D., D. L. Salzmann, L. B. Kleinert and S. K. Williams (2000). "Cellular proliferation and macrophage populations associated with implanted expanded polytetrafluoroethylene and polyethyleneterephthalate." J Biomed Mater Res 49(4): 489-497.

Harris, P. L., S. R. Vallabhaneni, P. Desgranges, J. P. Becquemin, C. van Marrewijk and R. J. Laheij (2000). "Incidence and risk factors of late rupture, conversion, and death after endovascular repair of infrarenal aortic aneurysms: the EUROSTAR experience. European Collaborators on Stent/graft techniques for aortic aneurysm repair." J Vasc Surg 32(4): 739-749.

Howell, M. H., M. Zaqqa, R. P. Villareal, N. E. Strickman and Z. Krajcer (2000). "Endovascular exclusion of abdominal aortic aneurysms: initial experience with stent-grafts in cardiology practice." Tex Heart Inst J 27(2): 136-145.

Izzat, M. B., D. Mehta, A. J. Bryan, B. Reeves, A. C. Newby and G. D. Angelini (1996). "Influence of external stent size on early medial and neointimal thickening in a pig model of saphenous vein bypass grafting." Circulation 94(7): 1741-1745.

Jayia, P., J. Constantinou, L. Morgan-Rowe, T. V. Schroeder, L. Lonn and K. Ivancev (2013). "Are there fewer complications with third generation endografts in endovascular aneurysm repair?" J Cardiovasc Surg (Torino) 54(1): 133-143.

Jones, J. A., D. T. Chang, H. Meyerson, E. Colton, I. K. Kwon, T. Matsuda and J. M. Anderson (2007). "Proteomic analysis and quantification of cytokines and chemokines from biomaterial surface-adherent macrophages and foreign body giant cells." J Biomed Mater Res A 83(3): 585-596.

Jones, J. A., A. K. McNally, D. T. Chang, L. A. Qin, H. Meyerson, E. Colton, I. L. Kwon, T. Matsuda and J. M. Anderson (2008). "Matrix metalloproteinases and their inhibitors in the foreign body reaction on biomaterials." J Biomed Mater Res A 84(1): 158-166.

Jung, M., M. S. Lord, B. Cheng, J. G. Lyons, H. Alkhouri, J. M. Hughes, S. J. McCarthy, R. V. Iozzo and J. M. Whitelock (2013). "Mast Cells Produce Novel Shorter Forms of Perlecan That Contain Functional Endorepellin: A ROLE IN ANGIOGENESIS AND WOUND HEALING." J Biol Chem 288(5): 3289-3304.

Kasirajan, K., M. D. Dake, A. Lumsden, J. Bavaria and M. S. Makaroun (2012). "Incidence and outcomes after infolding or collapse of thoracic stent grafts." J Vasc Surg 55(3): 652-658; discussion 658.

Khurana, R., Z. Zhuang, S. Bhardwaj, M. Murakami, E. De Muinck, S. Yla-Herttuala, N. Ferrara, J. F. Martin, I. Zachary and M. Simons (2004). "Angiogenesis-dependent and independent phases of intimal hyperplasia." Circulation 110(16): 2436-2443.

Kim, W. H., Y. G. Ko, K. W. Kang, J. S. Kim, B. K. Kim, D. Choi, M. K. Hong and Y. Jang (2012). "Effects of combination therapy with celecoxib and doxycycline on neointimal hyperplasia and inflammatory biomarkers in coronary artery disease patients treated with bare metal stents." Yonsei Med J 53(1): 68-75.

Knolle, J. (1988). "[Immunohistochemical characterization of epithelioid cells]." Acta Histochem Suppl 35: 159-164.

Koskas, F., I. Brocheriou, P. Cluzel, J. D. Singland, B. Regnier, M. Bonnot and E. Kieffer (2005). "Custom-made stent-grafts for aortic aneurysm repair using gianturco Z stents and woven polyester: healing in an animal model." Vasc Endovascular Surg 39(1): 55-65.

Koskas, F., P. Cluzel, A. C. Benhamou and E. Kieffer (1999). "Endovascular treatment of aortoiliac aneurysms: made-to-measure stent-grafts increase feasibility." Ann Vasc Surg 13(3): 239-246.

Langhans, T. (1868). "Über Riesenzellen mit wandständigen Kernen in Tuberkeln und die fibröse Form des Tuberkels." Arch Pathol Anat 42:: 382–404.

Le Manach, Y., C. Ibanez Esteves, M. Bertrand, J. P. Goarin, M. H. Fleron, P. Coriat, F. Koskas, B. Riou and P. Landais (2011). "Impact of preoperative statin therapy on adverse postoperative outcomes in patients undergoing vascular surgery." Anesthesiology 114(1): 98-104.

Lederle, F. A., J. A. Freischlag, T. C. Kyriakides, J. S. Matsumura, F. T. Padberg, Jr., T. R. Kohler, P. Kougias, J. M. Jean-Claude, D. F. Cikrit, K. M. Swanson and O. V. A. C. S. Group (2012). "Long-term comparison of endovascular and open repair of abdominal aortic aneurysm." N Engl J Med 367(21): 1988-1997.

Lindholt, J. S. (2001). "Screening for abdominal aortic aneurysm." Br J Surg 88(5): 625-626.

Lindholt, J. S. (2003). "Screening for abdominal aortic aneurysms." Eur J Vasc Endovasc Surg 25(5): 377-379.

Lohoefer, F., C. Reeps, C. Lipp, M. Rudelius, A. Zimmermann, S. Ockert, H. H. Eckstein and J. Pelisek (2012). "Histopathological analysis of cellular localization of cathepsins in abdominal aortic aneurysm wall." Int J Exp Pathol 93(4): 252-258.

MacLauchlan, S., E. A. Skokos, N. Meznarich, D. H. Zhu, S. Raoof, J. M. Shipley, R. M. Senior, P. Bornstein and T. R. Kyriakides (2009). "Macrophage fusion, giant cell formation, and the foreign body response require matrix metalloproteinase 9." Journal of Leukocyte Biology 85(4): 617-626.

Maier, A., M. W. Gee, C. Reeps, J. Pongratz, H. H. Eckstein and W. A. Wall (2010). "A comparison of diameter, wall stress, and rupture potential index for abdominal aortic aneurysm rupture risk prediction." Ann Biomed Eng 38(10): 3124-3134.

Major, A., R. Guidoin, G. Soulez, L. A. Gaboury, G. Cloutier, M. Sapoval, Y. Douville, G. Dionne, R. H. Geelkerken, P. Petrasek and S. Lerouge (2006). "Implant Degradation

and Poor Healing After Endovascular Repair of Abdominal Aortic Aneurysms: An Analysis of Explanted Stent-Grafts." Journal of Endovascular Therapy 13(4): 457-467.

McNally, A. K. and J. M. Anderson (1995). "Interleukin-4 induces foreign body giant cells from human monocytes/macrophages. Differential lymphokine regulation of macrophage fusion leads to morphological variants of multinucleated giant cells." Am J Pathol 147(5): 1487-1499.

McNally, A. K. and J. M. Anderson (2011). "Foreign body-type multinucleated giant cells induced by interleukin-4 express select lymphocyte co-stimulatory molecules and are phenotypically distinct from osteoclasts and dendritic cells." Exp Mol Pathol 91(3): 673-681.

Mehrpooya, M., M. Salehi, R. Eskandari, Z. Shajirat, A. Golabchi and M. Mazoochi (2012). "Diagnostic dilemma: Saccular aneurysm or pseudoaneurysm of the ascending aorta with dissection above level of leaflets." ARYA Atheroscler 8(3): 167-169.

Merino, V. F., M. Todiras, M. A. Mori, V. M. Sales, R. G. Fonseca, V. Saul, K. Tenner, M. Bader and J. B. Pesquero (2009). "Predisposition to atherosclerosis and aortic aneurysms in mice deficient in kinin B1 receptor and apolipoprotein E." J Mol Med (Berl) 87(10): 953-963.

Mestres, G., J. P. Uribe, C. Garcia-Madrid, E. Miret, X. Alomar, M. Burrell and V. Riambau (2012). "The best conditions for parallel stenting during EVAR: an in vitro study." Eur J Vasc Endovasc Surg 44(5): 468-473.

Molacek, J., V. Treska, J. Kobr, B. Certik, T. Skalicky, V. Kuntscher and V. Krizkova (2009). "Optimization of the model of abdominal aortic aneurysm--experiment in an animal model." J Vasc Res 46(1): 1-5.

Most, J., L. Spotl, G. Mayr, A. Gasser, A. Sarti and M. P. Dierich (1997). "Formation of multinucleated giant cells in vitro is dependent on the stage of monocyte to macrophage maturation." Blood 89(2): 662-671.

Oberhuber, A., M. Buecken, M. Hoffmann, K. H. Orend and B. M. Muhling (2012). "Comparison of aortic neck dilatation after open and endovascular repair of abdominal aortic aneurysm." J Vasc Surg 55(4): 929-934.

Okamoto, H., K. Mizuno and T. Horio (2003). "Langhans-type and foreign-body-type multinucleated giant cells in cutaneous lesions of sarcoidosis." Acta Derm Venereol 83(3): 171-174.

Pappu, S., A. Dardik, H. Tagare and R. J. Gusberg (2008). "Beyond fusiform and saccular: a novel quantitative tortuosity index may help classify aneurysm shape and predict aneurysm rupture potential." Ann Vasc Surg 22(1): 88-97.

Parodi, J. C., J. C. Palmaz and H. D. Barone (1991). "Transfemoral intraluminal graft implantation for abdominal aortic aneurysms." Ann Vasc Surg 5(6): 491-499.

Pearce, W. H. and V. P. Shively (2006). "Abdominal aortic aneurysm as a complex multifactorial disease: interactions of polymorphisms of inflammatory genes, features of autoimmunity, and current status of MMPs." Ann N Y Acad Sci 1085: 117-132.

Prinssen, M., E. L. Verhoeven, J. Buth, P. W. Cuypers, M. R. van Sambeek, R. Balm, E. Buskens, D. E. Grobbee, J. D. Blankensteijn and G. Dutch Randomized Endovascular Aneurysm Management Trial (2004). "A randomized trial comparing conventional and endovascular repair of abdominal aortic aneurysms." N Engl J Med 351(16): 1607-1618.

Reeps, C., J. Pelisek, S. Seidl, T. Schuster, A. Zimmermann, A. Kuehnl and H. H. Eckstein (2009). "Inflammatory infiltrates and neovessels are relevant sources of MMPs in abdominal aortic aneurysm wall." Pathobiology 76(5): 243-252.

Satoh, K., P. Nigro, T. Matoba, M. R. O'Dell, Z. Cui, X. Shi, A. Mohan, C. Yan, J. Abe, K. A. Illig and B. C. Berk (2009). "Cyclophilin A enhances vascular oxidative stress and the development of angiotensin II-induced aortic aneurysms." Nat Med 15(6): 649-656.

Scheumann, J., C. Heilmann, F. Beyersdorf, M. Siepe, R. M. Brenner, D. Bockler, R. B. Griepp and M. S. Bischoff (2012). "Early histological changes in the porcine aortic media after thoracic stent-graft implantation." J Endovasc Ther 19(3): 363-369.

Schlaweck, S., S. Zimmer, R. Struck, E. Bartok, N. Werner, F. Bauernfeind, E. Latz, G. Nickenig, V. Hornung and A. Ghanem (2011). "Critical role of nucleotide-binding oligomerization domain-like receptor 3 in vascular repair." Biochem Biophys Res Commun 411(3): 627-631.

Schurmann, K., D. Vorwerk, A. Bucker, J. Neuerburg, B. Klosterhalfen, G. Muller, R. Uppenkamp and R. W. Gunther (1997). "Perigraft inflammation due to Dacron-covered stent-grafts in sheep iliac arteries: correlation of MR imaging and histopathologic findings." Radiology 204(3): 757-763.

Siegenthaler, M. P., R. Celik, J. Haberstroh, P. Bajona, H. Goebel, K. Brehm, W. Euringer and F. Beyersdorf (2008). "Thoracic endovascular stent grafting inhibits aortic growth: an experimental study." Eur J Cardiothorac Surg 34(1): 17-24.

Singland, J. D., D. Mitton, A. Guillaume, P. Cluzel, P. Goasdoue, F. Lavaste, E. Kieffer and F. Koskas (2010). "Dynamics of homemade aortic endografts: in vivo study in humans with computed tomography scanner modeling." Ann Vasc Surg 24(1): 127-139.

Svensjo, S., H. Bengtsson and D. Bergqvist (1996). "Thoracic and thoracoabdominal aortic aneurysm and dissection: an investigation based on autopsy." Br J Surg 83(1): 68-71.

Swedenborg, J., M. I. Mayranpaa and P. T. Kovanen (2011). "Mast cells: important players in the orchestrated pathogenesis of abdominal aortic aneurysms." Arterioscler Thromb Vasc Biol 31(4): 734-740.

Thun, M. J., B. D. Carter, D. Feskanich, N. D. Freedman, R. Prentice, A. D. Lopez, P. Hartge and S. M. Gapstur (2013). "50-year trends in smoking-related mortality in the United States." N Engl J Med 368(4): 351-364.

Trollope, A., J. V. Moxon, C. S. Moran and J. Golledge (2011). "Animal models of abdominal aortic aneurysm and their role in furthering management of human disease." Cardiovasc Pathol 20(2): 114-123.

Ueberrueck, T., J. Tautenhahn, L. Meyer, O. Kaufmann, H. Lippert, I. Gastinger and T. Wahlers (2005). "Comparison of the ovine and porcine animal models for biocompatibility testing of vascular prostheses." J Surg Res 124(2): 305-311.

van der Bas, J. M., P. H. Quax, A. C. van den Berg, M. J. Visser, E. van der Linden and J. H. van Bockel (2004). "Ingrowth of aorta wall into stent grafts impregnated with basic fibroblast growth factor: a porcine in vivo study of blood vessel prosthesis healing." J Vasc Surg 39(4): 850-858.

van Prehn, J., F. J. Schlosser, B. E. Muhs, H. J. Verhagen, F. L. Moll and J. A. van Herwaarden (2009). "Oversizing of aortic stent grafts for abdominal aneurysm repair: a systematic review of the benefits and risks." Eur J Vasc Endovasc Surg 38(1): 42-53.

Wanhainen, A. (2008). "How to define an abdominal aortic aneurysm--influence on epidemiology and clinical practice." Scand J Surg 97(2): 105-109; discussion 109.

White, J. G., N. J. Mulligan, D. R. Gorin, R. D'Agostino, E. K. Yucel and J. O. Menzoian (1998). "Response of normal aorta to endovascular grafting: a serial histopathological study." Arch Surg 133(3): 246-249.

Yavuz, K., S. Geyik, D. Pavcnik, B. T. Uchida, C. L. Corless, D. E. Hartley, A. Goktay, L. O. Correa, H. Timmermans, J. P. Hodde, J. A. Kaufman, F. S. Keller and J. Rosch (2006). "Comparison of the endothelialization of small intestinal submucosa, dacron, and expanded polytetrafluoroethylene suspended in the thoracoabdominal aorta in sheep." J Vasc Interv Radiol 17(5): 873-882.

Zankl, A. R., H. Schumacher, U. Krumsdorf, H. A. Katus, L. Jahn and C. P. Tiefenbacher (2007). "Pathology, natural history and treatment of abdominal aortic aneurysms." Clin Res Cardiol 96(3): 140-151.

8 Index of tables

9 Index of figures

10 Attachments

Attachment 1 HES staining protocol

AP-HP Groupe hospitalier PITIE-SALPETRIERE
Service d'anatomie et cytologie pathologiques
Pr F.Capron

GUIDE DES BONNES PRATIQUES
Référence : COLO.026/A

COLORATION A L'HEMATEINE EOSINE SAFRAN (HES)

Objet : Création **Indice :** A **Date:20/12/2004**

	Nom	Fonction	Visa	Date
REDACTEUR	F.DE Trazegnies	Technicien de laboratoire		14/01/03 17:32
VALIDATION par:	F.Capron	Chef de service		

TECHNIQUE

- Coupes déparaffinées et amenées à l'eau (cf. procédure de déparaffinage)
- **Hemalun de Mayer** : 3'
- Laver à l'eau
- **Acide chlorhydrique à 2%** : 10"
- Eau
- **Alcool 70 ammoniacal à 3%** : 15" (Alcool 70° 970 ml – Ammoniaque concentré 30ml)
- Rincer à l'eau
- **Solution d'éosine** : 2'
- -Rincer à l'eau
- Alcool absolu
- **Safran** : 2'
- Alcool absolu x2
- Xylène x2
- Montage au Pertex

RESULTATS

Noyaux bleu-violet
Cytoplasme rouge
Collagène Jaune-orange

REACTIFS

Hémalun de Mayer modifié:
solution du commerce (RAL) dans laquelle on ajoute 20cc d'acide acétique concentré par litre

Solution d'Eosine

Eosine jaunâtre : 10g
Erythrosine B : 10g
Orange G : 5g
Eau distillée 1000ml

Eosine Jaunâtre = Eosine Y

Safran

Sécher à l'étuve à 56° 20g de filaments de safran pendant 1 semaine
A l'aide d'un mortier , écraser les filaments séchés et y ajouter 1 litre d'alcool absolu
Cette solution se conserve à l'étuve

Attachment 2 WHPS staining protocol

AP-HP Groupe hospitalier PITIE-SALPETRIERE
Service d'anatomie et cytologie pathologiques
Pr F.Capron

COLORATION DE WEIGERT HEMALUN-PHLOXINE-SAFRAN

Objet :Création Indice :A Date:20/12/2004

	Nom	Fonction	Visa	Date
REDACTEUR	F.De Trazegnies	Techniciens de laboratoire		14/01/03 17:32
VALIDATION par:	Pr F.Capron	Chef de service		

TECHNIQUE :

- Coupes déparaffinées et amenées à l'eau (cf. procédure de déparaffinage)
- Colorer dans la solution de **fuchsine résorcine**: 15' à 45'
- Laver à l'eau pendant quelques secondes
- Laver à l'eau distillée pendant 5 minutes.(on peut laisser les lames en attente dans l'eau)
- Différencier dans l'**alcool chlohydrique** pendant quelques secondes(jusqu'à ce que
- tout l'excès de colorant soit éliminé)
- Laver à l'eau distillée
- Colorer dans l'hémalun pendant 3mn
- Laver à l'eau courante
- Décolorer dans **HCL 1%** dans l'eau distillée
- Rincer à l'eau courante
- Bleuir dans **NH4 à 3%** dans l'alcool à 70°
- Rincer à l'eau distillée
- Colorer dans une solution de **phloxine à 3%** dans de l'eau distillée pendant 1mn
- Rincer à l'eau courante
- Différencier dans de **l'alcool 100°**
- Colorer par du **safran en solution alcoolique** pendant 3mn
- Rincer rapidement par une jet de pissette d'alcool 100°
- Passer très rapidement dans l'alcool 100°
- Xylène
- Montage au Pertex

RESULTATS :

- Fibres élastiques : violet foncé
- Noyaux : bleus
- Cytoplasmes : roses
- Collagène : jaune d'or

EACTIFS :

Fuschine résorcine : prête à l'emploi

Attachment 3 Protocol of aortic layer measurement

	Clearpass protocol 1				date:					
	investigator:									
	sheep		stent position							
	pathono:		neointima	media	neointima+media	summe		ratio	pic no:	
		1measure								
	sample site:	2 measure								
		3measure								
	pathono:		intima	media	intima+media	summe		ratio	pic no:	
		1measure								
	sample site:	2 measure								
		3measure								
	Observation:									

Attachment 4 Media rupture and angiogenesis protocol

	Clear pass protocol 2				date:						
	investigator:										
	sheep		stent position								
	pathono:		MLU not-stented	pathono:		MLU stented	%	loss of undulation	rupture score	pic no:	
		1measure			1measure						
	sample site:	2 measure		sample site:	2 measure						
		3measure			3measure						
	Observation:										
	pathono:		pathono:				pathono:		pathono:		
	sheep		sheep				sheep		sheep		
	stentposition		stentposition				stentposition		stentposition		
	Vessels counted		Vessels counted				CD3+ cell count		CD3+ cell count		
	luminal	parietal	luminal	parietal			luminal	parietal	luminal	parietal	

11 Eidesstattliche Versicherung

„Ich, Kraas, Luise, versichere an Eides statt durch meine eigenhändige Unterschrift, dass ich die vorgelegte Dissertation mit dem Thema: „Inflammation and mechanical injury as possible reasons for chronic graft failure: A histological analysis of chrome-cobalt stent grafts in the sheep aorta" selbstständig und ohne nicht offengelegte Hilfe Dritter verfasst und keine anderen als die angegebenen Quellen und Hilfsmittel genutzt habe.
Alle Stellen, die wörtlich oder dem Sinne nach auf Publikationen oder Vorträgen anderer Autoren beruhen, sind als solche in korrekter Zitierung (siehe „Uniform Requirements for Manuscripts (URM)" des ICMJE - *www.**icmje**.org*) kenntlich gemacht. Die Abschnitte zu Methodik (insbesondere praktische Arbeiten, Laborbestimmungen, statistische Aufarbeitung) und Resultaten (insbesondere Abbildungen, Graphiken und Tabellen) entsprechen den URM (s.o) und werden von mir verantwortet.
Meine Anteile an etwaigen Publikationen zu dieser Dissertation entsprechen denen, die in der untenstehenden gemeinsamen Erklärung mit dem/der Betreuer/in, angegeben sind. Sämtliche Publikationen, die aus dieser Dissertation hervorgegangen sind und bei denen ich Autor bin, entsprechen den URM (s.o) und werden von mir verantwortet.

Die Bedeutung dieser eidesstattlichen Versicherung und die strafrechtlichen Folgen einer unwahren eidesstattlichen Versicherung (§156,161 des Strafgesetzbuches) sind mir bekannt und bewusst."

Datum Unterschrift

12 Curriculum vitae

Acknowledgments

I wish to express my sincere gratitude to all those who have helped me to finish this dissertation.
To Prof. Dr. Ulrich Speck, Institut für Radiologie, Charité-Universitätsmedizin Berlin I am indebted and grateful for his role as my academic Doktorvater in Berlin.
To Prof. Fabian Koskas, Head of the department of Vascular Surgery, Hôpital Pitié-Salpêtrière, Université Pierre et Marie Curie Paris VI, I thank for the opportunity to train and work in his department and for providing the research facilities. Both his enthusiasm to advance surgical techniques as well as his calm, compassionate and precise surgical routine have been an inspiration.
To Dr. Peter Dorfmüller, Hôpital Marie Lannelongue, I am thankful for introducing me to the field of pathology and help me with the histopathological assessment.

My stay in Paris was supported by the DAAD and a grant by the Bayerisch-Französisches Hochschulzentrum. I am thankful to both institutions for the opportunity to do medical research and training in Paris. The experience has been invaluable.